

Dalton Transactions

Accepted Manuscript



This is an *Accepted Manuscript*, which has been through the Royal Society of Chemistry peer review process and has been accepted for publication.

Accepted Manuscripts are published online shortly after acceptance, before technical editing, formatting and proof reading. Using this free service, authors can make their results available to the community, in citable form, before we publish the edited article. We will replace this *Accepted Manuscript* with the edited and formatted *Advance Article* as soon as it is available.

You can find more information about *Accepted Manuscripts* in the [Information for Authors](#).

Please note that technical editing may introduce minor changes to the text and/or graphics, which may alter content. The journal's standard [Terms & Conditions](#) and the [Ethical guidelines](#) still apply. In no event shall the Royal Society of Chemistry be held responsible for any errors or omissions in this *Accepted Manuscript* or any consequences arising from the use of any information it contains.

Spectroscopic studies of lanthanide complexes of varying nuclearity based on a compartmentalised ligand

Daniela Olea-Román^a, Nicolas Bélanger-Desmarais^b, Marcos Flores-Álamo^a, Claudia Bazán^c, Félix Thouin^c, Christian Reber^{b,*}, Silvia E. Castillo-Blum^{a,*}

^aFacultad de Química, Universidad Nacional Autónoma de México, Ciudad Universitaria, Coyoacán, D. F. 04510. México.

^bDépartement de chimie, Université de Montréal, Montréal, QC H3C 3J7, Canada.

^cDépartement de physique, Université de Montréal, Montréal, QC H3C 3J7, Canada.

*blum@unam.mx, *christian.reber@umontreal.ca

Abstract

The synthesis, characterization and solid-state luminescence spectroscopy of mononuclear (*f*), heterodinuclear (*d-f*) and heterotrinnuclear (*d-f-d*) coordination compounds with the compartmental ligand N,N'-bis(3-hydroxyl salicylidene)benzene-1,2-diamine (*H₂L*) are reported. The trivalent lanthanide ions Nd^{III}, Sm^{III}, Eu^{III}, Gd^{III}, Tb^{III} and Dy^{III} as single metal centres or in combination with either Zn^{II} or Ni^{II} were coordinated. Compounds are characterised by elemental analyses, IR, 1D and 2D solution ¹H and ¹³C NMR spectroscopy, measurements of magnetic moments and solid state UV-Vis-NIR reflectance, luminescence and Raman spectroscopies. Crystal structures of the dinuclear compounds [*SmZn(O₂NO*)₃(*L*)(*OH*₂)]·*EtOH* and [*DyZn(O₂NO*)₂(*Cl*)(*L*)(*EtOH*)]·3*EtOH* and for the trinuclear [*TbZn₂(L)*]₂(*Cl*)₂(*OH*₂)](*NO*₃)·*EtOH* are presented, where samarium(III) displays a coordination number of ten, with a bicapped cubic geometry, while for the dysprosium compound a nine-coordinated environment with a tricapped trigonal prismatic geometry is shown. Their crystals belong to the triclinic system and P-1 space group. The coordination number for terbium(III) in the trinuclear complex is nine, with a tricapped trigonal prismatic geometry, and its crystal belongs to the monoclinic system, space group C2/c. For these three compounds, the zinc ion stabilises a penta-coordinated environment with square pyramid geometry. All mononuclear and dinuclear compounds are neutral, whereas the trinuclear complexes are ionic. Results of DFT theoretical calculations for the ligand (*H₂L*) are used to assign the ligand singlet and triplet excited state energy levels. Luminescence studies of the neodymium compounds indicate that the ligand is a sensitizer for the NIR emitters.

Keywords: Vibrational Spectroscopies, UV-Vis-NIR absorption, Luminescence, Compartmental Schiff-Base, *d-f* hybrid complexes.

Introduction

Lanthanide ions doped in crystal lattices and molecular lanthanide compounds show a wide variety of luminescence properties, and are a long-standing focus of research interest in the last decades¹⁻³ partly due to their applications as phosphors and luminescent materials. More recently, molecular and nanoscale lanthanide systems have been proposed as luminescent probes both in biosciences as well as in materials science.⁴⁻¹⁰

Near-infrared (NIR) emitting lanthanide ions such as Nd^{III}, Er^{III} and Yb^{III} are of interest, as shown by the significant increase in the number of publications due to their numerous potential applications which range from biomolecular labelling in luminescent bioassays to functional materials for optical telecommunication networks,¹⁰⁻¹⁷ and more recently as molecular thermometers.¹⁸

Nevertheless, *f-f* transitions are parity forbidden; therefore direct excitation into the 4*f* excited levels rarely yields highly luminescent materials. To overcome this situation, sensitization of the luminescence by energy transfer has been achieved, for example by coordinating the metal ion to a chromophore.¹⁹ This chromophore, a good light harvester, may be an organic ligand or a transition metal coordination compound and acts as an antenna.²⁰⁻²⁵

A variety of ligands have been employed as sensitizers, containing N or O donor atoms, such as aromatic carboxylic acids, aromatic imines, β -diketones, and many others.²⁶⁻³⁰

The design of ligands that yields stable and substitution inert coordination compounds with lanthanides and, at the same time, act as efficient antenna has seen a tremendous development during the past two decades.⁴ Among them, Schiff bases have been successfully employed as ligands both for the *d*- and *f*-blocks metal ions; even more, if an adequate design is carried out, compartmental ligands can be synthesised which may be able to coordinate two or more metal ions.^{31,32} It is worth to mention that the utilization of this type of ligands as antenna groups for lanthanides has also been reported.^{33,34}

To devise chromophores which may work as efficient antennae for lanthanide ions is a fundamental task. It is important to consider and achieve an optimum coupling between the electronic excited states of the chromophore with the emissive levels of the lanthanide ion. For

Eu^{III} and Tb^{III} it has been reported that the ideal energy gap between the triplet state of the chromophore and the emissive level of the lanthanide lies between 2000 and 4000 cm⁻¹.⁴ Sensitization of the luminescence of NIR-emitting Ln^{III} ions may involve the energy transfer from both singlet and triplet excited states of the ligand to the emissive level of the metal ion, particularly for the ions having several excited electronic levels above 30 000 cm⁻¹.³⁵ Modern computational methods, combined with experimental spectroscopic properties of lanthanides have aided scientists to design highly luminescent materials; particularly since the understanding of the spectroscopic properties of these ions has advanced in the last decades.¹ However, there is still a need to improve theoretical calculations to get quantitatively reliable predictions of photophysical properties. In this manuscript we report the synthesis of mononuclear, heterodinuclear (*d-f*) and heterotrinnuclear (*d-f-d*) coordination compounds containing Nd^{III}, Sm^{III}, Eu^{III}, Gd^{III}, Tb^{III} and Dy^{III}, and Zn^{II} or Ni^{II} with the Schiff base N,N'-bis(3-hydroxyl salicylidene)benzene-1,2-diamine, their characterisation, including X-ray crystal structures of three heteronuclear coordination compounds. We studied the solid-state luminescence of these compounds and their Raman spectra. Results of DFT theoretical calculations for the ligand (*H₂L*) are also presented.

Results and Discussion

Synthesis

The solid starting materials (*o*-phenylenediamine and 2,3-dihydroxybenzaldehyde) were mixed and then the solvent was added giving a yellow solution by stirring the mixture. From this solution a red crystalline precipitate is formed on heating, which corresponds to the Schiff base, *H₂L*. It was obtained in high yield and as a pure product, characterized by elemental analysis, IR, Raman, NMR spectroscopies. The Schiff base itself acts as sensitizer for the lanthanide ions. Also, coordination compounds with *d*-block ions (Ni^{II} and Zn^{II}) were prepared to use them as antenna groups for lanthanides. The reaction synthesis using either the nickel(II) chloride or nitrate salts generated terracotta precipitates of the coordination compound [*NiL*] in high yield. The antenna was obtained from an ethanolic hot solution of the ligand to which the metal salt was added and this reaction mixture was stirred for an hour. The same synthetic method was

carried out for the zinc(II) compound and the yields observed in this case were lower than those for the corresponding nickel(II) compounds.

Vibrational spectroscopy

IR and Raman spectra show characteristic frequencies in the region of the coordination site.

Some important IR absorptions of H_2L were assigned to the $\nu_{C=N}$ stretching vibration at 1611 cm^{-1} , the strong vibration due to ν_{O-H} at 3467 cm^{-1} and a weak absorption at 3053 cm^{-1} due to ν_{N-C-H} vibration, ν_{C-O} at 1272 cm^{-1} and δ_{C-O-H} at 1480 cm^{-1} .³⁶ The corresponding Raman frequencies are similar; all frequencies are given in Table 1. Experimental and calculated (DFT) vibrational spectra are given as ESI. Calculated spectra are in good agreement with experimental data. As an example, the mode at 1611 cm^{-1} (IR, Raman) involves the two C=N oscillators and has antisymmetric C=N stretching character calculated for the IR frequency at 1660.8 cm^{-1} and symmetric C=N stretching character for the 1661.1 cm^{-1} calculated Raman frequency.

In the IR spectra of the mononuclear $[Ln(O_2NO)_3(H_2L)] \cdot n(H_2O)$ and the dinuclear complexes $[LnZn(O_2NO)_2(Cl)(L)(OH_2)] \cdot nH_2O$ the characteristic vibrations of the coordinating nitrate groups (C_{2v}) at *ca.* 1484 cm^{-1} (ν_1), 1300 cm^{-1} (ν_4), 1045 cm^{-1} (ν_2) and 812 cm^{-1} (ν_3) were observed; while the difference in the frequency positions of the nitrate vibrations between the two strongest absorptions (ν_1 and ν_4) is around 180 cm^{-1} , indicating that the NO_3^- groups are coordinating in a bidentate fashion.^{37,38} Additionally, it was observed that the characteristic absorptions of H_2L are shifted upon coordination to the metal ions. The $\nu_{C=N}$ stretching vibration is observed between 1610 cm^{-1} and 1618 cm^{-1} , the weak absorption due to ν_{N-C-H} vibration appears between 3054 cm^{-1} and 3064 cm^{-1} , while that assigned to the ν_{C-O} vibration is observed from 1247 cm^{-1} to 1263 cm^{-1} ; indicating that the ligand is coordinated through the N_2O_2 tetragonal base to the transition metal ion and the four oxygen atoms, two of them from the phenolato groups, and the remaining from the -OH groups arising from the Schiff base to the lanthanide metal ion.

The IR spectra of the trinuclear complexes $[LnNi_2(L)_2(Cl)]Cl(NO_3) \cdot nH_2O$ only showed the characteristic vibrations of the free nitrate groups around 1380 cm^{-1} , 820 cm^{-1} and 730 cm^{-1} , while those due to the presence of the coordinated Schiff base were shifted from their position in the uncoordinated ligand, see Table 1.

Magnetic Moments of the coordination compounds

The effective magnetic moments of all coordination compounds were obtained by the Gouy method and correspond to the expected values for the lanthanide(III) ions, see Table 1. It can therefore be concluded that nickel(II) does not contribute to the paramagnetism of the complexes, therefore this ion is diamagnetic, with a square planar coordination geometry.

Electrical Conductivity

The conductivity measurements of 1×10^{-3} M DMF solutions of the trinuclear complexes indicate that they are 1:2 electrolytes. On the other hand, their IR spectra suggest that the nitrate ion acts as counterion, therefore the second anion is likely a chloride ion.

NMR Spectra

The unequivocal assignment of the ^1H and ^{13}C NMR spectra was carried using the 2D HSQC ^1H - ^{13}C and COSY ^1H - ^1H experiments, see Experimental and ESI sections. It is worth to mention that the proton attached to the oxygen atoms from the phenol group was not observed in the spectra of the nickel(II) or zinc(II) compounds, indicating that the ligand lost two protons upon coordination. All the proton signals were shifted in the spectra of the coordination compounds compared to their position in the Schiff base. The signals for H-9 and H-10 appeared as a multiplet in the spectrum of the ligand, while they were observed at two different chemical shifts in the spectrum of either $[\text{NiL}]$ or $[\text{ZnL}(\text{OH}_2)]$. In a similar manner, the position of the C atoms was shifted in the ^{13}C NMR spectra of the coordination compounds as compared with that of the chromophore spectrum, the larger effect was observed for C-1, C-2 and C-7, neighbouring atoms of the N_2O_2 coordinating tetragonal base.

In all cases, the proposed molecular formulae are in accordance with the elemental analyses data (see experimental section).

Crystal structures

The structures $[\text{DyZn}(\text{O}_2\text{NO})_2(\text{Cl})(\text{L})(\text{EtOH})] \cdot 3(\text{EtOH})$ (**15a**), $[\text{SmZn}(\text{O}_2\text{NO})_3(\text{L})(\text{OH}_2)] \cdot \text{EtOH}$ (**16**) and $[\text{TbZn}_2(\text{L})_2(\text{Cl})_2(\text{OH}_2)](\text{NO}_3) \cdot \text{EtOH}$ (**23**) were determined by X-ray diffraction, with crystallographic parameters, data collection, and refinements summarized in Table 2. CCDC: 1409844 (**15a**), 1409843 (**16**) and 1409842 (**23**) Selected bond lengths and angles for the three

compounds **15a**, **16** and **23** are given in Tables 3, 4, 5, respectively. Perspective views of the dinuclear compounds **15a** and **16** and trinuclear Zn₂/Tb **23** complex are given as Figs. 1-3.

The $[DyZn(O_2NO)_2(Cl)(L)(EtOH)] \cdot 3EtOH$ dinuclear Zn-Dy neutral complex **15a** (Fig. 1) consists of one Zn^{II} ion bonded to the inner N, N', O, O' core of one of the Schiff-base ligands with a slight distorted square pyramidal geometry similar to **16** and **23** compounds, this penta-coordinated metal atom has the axial site occupied by one chloride, the Dy^{III} metal ion is coordinated to four oxygen atoms from the Schiff base, two bidentate nitrates and one ethanol molecule. Three crystallisation ethanol molecules, one of them disordered, are also present.

The geometry around the Zn^{II} ion can be described as a perfect square-pyramidal geometry with a τ parameter of 0.002, where the zinc metal atom lays 0.55 Å above the plane formed by N10/N17/O8/O19. The Zn-Dy distance of 3.5003(8) Å is consistent with the dinuclear complex reported (3.490 Å)³⁹ and shorter to the trinuclear analogue compounds (3.616 Å).³²

The typical eight-coordination of the Dy^{III} metal ion is observed in other analogue dinuclear and trinuclear complexes.³² Nine-coordinated mononuclear dysprosium(III) complexes where the geometry around the metal ion is either pseudo-monocapped square antiprismatic, or a tricapped trigonal prismatic conformation have also been reported.^{40,41}

On the other hand, the $[SmZn(O_2NO)_3(L)(OH_2)] \cdot EtOH$ dinuclear Zn-Sm neutral complex **16** (Fig. 2) consists of one Zn^{II} ion bonded to the inner N, N', O, O' core of one unit of the Schiff-base ligand and to a fifth coordinated oxygen atom from a water molecule; while the ten-coordinated Sm^{III} ion is coordinated to four oxygen atoms of the Schiff-base ligand and six oxygen atoms of three nitrate anions. One disordered crystallisation ethanol molecule is also observed. The geometry around the Zn^{II} ion can be described as slightly distorted square-pyramid, where the τ parameter is of 0.06 and the zinc metal atom lays 0.50 Å above the plane formed by N10/N17/O8/O19. The Zn-Sm distance of 3.5206(6) Å is shorter to the reported of 3.594 Å for analogue compounds.⁴² The typical ten-coordination of the Sm^{III} metal ion is also observed in similar compounds.⁴² The molecular geometry of this compound is further stabilised by intra and intermolecular hydrogen bond interactions. Intermolecular weak hydrogen bonds are observed between the nitrate oxygen atom of one molecule and the coordinated water from another molecule, and from the nitrate oxygen atoms and the disordered crystallisation ethanol molecule. Intermolecular hydrogen bonds are formed between O1 and the nitrate group.

In the trinuclear Zn^{II}/Tb **23** cationic complex, the discrete molecule $[TbZn_2(L)_2(Cl)_2(OH_2)](NO_3) \cdot EtOH$ (Fig. 3) consists of the two Zn^{II} ions bonded to the inner N, N', O, O' cores of the Schiff-base ligands, each Zn^{II} has one chloride as the fifth ligand occupying the axial site; while the Tb^{III} ion is coordinated to four oxygen atoms from the two Schiff-base ligands and one water molecule. The anion corresponds to one nitrate, disordered by symmetry; it also contains one crystallisation ethanol molecule. The geometry around each Zn^{II} ion can be described as a slightly distorted square-pyramidal,⁴³ for which a τ parameter of 0.03 was calculated; the zinc metal atom lies 0.467 Å above the plane formed by N1/N2/O2/O3. The Zn-Tb distance of 3.4972(4) Å is similar to that observed for the Zn-Tb dinuclear analogue compound, 3.485 Å, but is shorter to that of the trinuclear Zn-Tb-Zn analogue of 3.561 Å.³² The Tb^{III} ion is between the two ZnL units. The Tb^{III} metal centre in the trinuclear complex is nine-coordinated, surrounded by nine oxygen atoms; four from the phenolic groups, four hydroxyl groups (all of them from two different ligands) and one of the water molecule. Coordination geometry of the lanthanide ions in compounds **15a**, **16** and **23** are displayed as polyhedra in Fig. 4.

Powder diffraction

X-ray powder diffractograms of the dinuclear (**10** – **15**) and trinuclear (**17** – **22**) compounds families of coordination compounds were obtained. It was observed that the diffractograms for each family of complexes were very similar, indicating that within a family the compounds have the same unit cell. It is worth to emphasise that X-ray crystal structures of the dinuclear (**15a**) and trinuclear (**23**) compounds herein discussed contain crystallisation ethanol and that the calculated X-ray powder patterns for them were different from those of the powder samples. Elemental analyses of the powder samples indicate that the compounds contain crystallisation water instead of ethanol (see experimental section). Selected diffractograms are included in ESI.

Absorption and luminescence spectra

The solution absorption spectrum of H_2L in methanol (1×10^{-4} M) shows two intense absorption bands with maxima at 35088 cm^{-1} (285 nm) $\pi \rightarrow \pi^*$, a shoulder at 29940 cm^{-1} (334 nm) $n \rightarrow \pi^*$ and a weak band at 21367 cm^{-1} (468 nm) see Fig. 5, assigned to the S_1 to T_1 transition,⁴⁴ which

was confirmed by DFT calculations, see ESI for comparison experimental-calculated absorbance spectra.

The solid-state diffuse reflectance spectra of all compounds show intense, broad absorptions in the UV-region. The spectra of the chromophores and the lanthanide-based coordination compounds show similar features, maxima are identical within experimental precision.

Luminescence is observed from H_2L (**1**). The band maximum is at *ca.* 625 nm (*ca.* 16000 cm^{-1}) when the sample was excited at 488 nm, in the orange spectral region. Fig. 5 shows a comparison of absorption and luminescence spectra, confirming that the luminescence transition corresponds to the lowest-energy absorption band: electronic origin at *ca.* 21400 cm^{-1} , Stokes shift of 5367 cm^{-1} .

Luminescence bands with similar maxima and widths are observed for the mononuclear Sm^{III} , Eu^{III} , Gd^{III} , Tb^{III} and Dy^{III} compounds (Table 6), all spectra are shown in Fig. 6. It is noteworthy that f - f transitions are hidden by more intense features. In absorption or diffuse reflectance, the ligand spectrum with its onset at approximately 570 nm is more intense than f - f bands, therefore no f - f transitions at wavelengths shorter than 570 nm can be observed. And yet, diffuse reflectance bands due to f - f transitions at longer-wavelengths are observed for the Nd^{III} ⁴⁵ (Fig. 7), Sm^{III} ⁴⁶ and Dy^{III} ⁴⁸ compounds and the assignments are given in Table 6.

Nd^{III} compounds **4** and **10** show f - f luminescence⁴⁷ (Fig. 8). Luminescence spectra for the mononuclear **4** and dinuclear **10** compounds are shown in Fig. 9 at 80 K and room temperature; comparison with diffuse reflectance, allows identifying the well resolved transitions, see Table 6. The majority of the compounds prepared for this study show broad luminescence bands with maximum wavelengths summarized in Table 6. The uncoordinated ligand in its protonated form shows a similar broad luminescence band, illustrated in Fig. 5 in comparison to the absorption spectrum in the region of the lowest energy transition. This figure shows a typical mirror image relationship between absorption and luminescence bands⁴⁹, with a Stokes shift of approximately 5400 cm^{-1} separating the absorption maximum at 21400 cm^{-1} from the luminescence maximum at 16000 cm^{-1} . Adding one half of the Stokes shift to the energy of the luminescence maximum gives an estimate for the energy of the electronic origin, approximately 18700 cm^{-1} or 535 nm, corresponding very closely to the crossing point of the two spectra in Fig. 5. This comparison

shows that $f-f$ transitions are approximately 2000 cm^{-1} lower in energy than the absorption maximum should be observable and are possibly sensitized by the antenna.

DFT calculations help to elucidate the nature of this transition.⁵⁰ It has been assigned in the literature as a ligand centred π to π^* transition, and DFT calculations carried out for our ligand confirm this assignment. Plots of the HOMO and LUMO orbitals are given as ESI. Calculated UV-Vis absorption spectra are in very good agreement with the experimental solution absorption spectrum, a comparison also given in the ESI. The band maximum for the transition to the lowest-energy triplet excited state is calculated at 511 nm, in very good agreement with the experimental band maximum, as indicated in Fig. 5.

The detailed comparison of absorption and luminescence allows us to clearly state that no $f-f$ luminescence transitions at wavelengths shorter than 600 nm should be observed, as Kasha's rule states that luminescence occurs from the lowest energy state, where the difference between ligand T_1 and the emissive states of the lanthanides should be between 2500 and 3500 cm^{-1} .^{51,52} This energy consideration explains the absence of $f-f$ luminescence transitions for example, from Eu^{III} and Tb^{III} .

There are $f-f$ transitions expected lower in energy than the ligand-centered band for several compounds studied here. A comparison with Dieke's diagram⁵³ indicates that Nd^{III} luminescence should be observable and that Sm^{III} and Dy^{III} have non-emitting excited states below the energy threshold, therefore observable as absorption transitions. These transitions are listed for the Sm^{III} and Dy^{III} compounds in Table 6 and can be assigned by comparisons with literature spectra.^{48,49} In agreement with Dieke's diagram, no luminescence transitions are observed for these compounds.

The two Nd^{III} complexes, **4** and **10**, show NIR luminescence transitions. Fig. 8 shows overview spectra of solid samples at room temperature, clearly showing the ${}^4\text{F}_{3/2}$ to ${}^4\text{I}_{9/2}$ and ${}^4\text{F}_{3/2}$ to ${}^4\text{I}_{11/2}$ band systems. Overall widths of the two bands are 38 and 25 nm, respectively; compared to the published solution spectrum for a tetranuclear complex in solution which is of 76 nm.⁵⁴ Our detector sensitivity limit did not allow us to observe the ${}^4\text{F}_{3/2}$ to ${}^4\text{I}_{13/2}$ band system expected at wavelengths longer than 1300 nm. The two band systems observed clearly correspond to the Nd^{III} transitions and show resolved fine structure.

Luminescence lifetime of **4** is $(0.17 \pm 0.08) \mu\text{s}$, while that for the NdZn compound **10** is $(0.06 \pm 0.02) \mu\text{s}$. The dinuclear compound contains one coordination water molecule, which may cause a decrease in the lifetime value. The lifetime for the trinuclear compound **17** is $(0.00024 \pm 0.00004) \mu\text{s}$. Moreover, it is important to point out that the lifetime of the uncoordinated ligand is $(0.00031 \pm 0.000002) \mu\text{s}$, while that of $[\text{ZnL}(\text{OH}_2)]$ (**3**) is $(0.00033 \pm 0.000002) \mu\text{s}$ and for $[\text{NiL}]$ (**2**) is $(0.00023 \pm 0.00002) \mu\text{s}$. The transition that was monitored for the three neodymium(III) compounds was ${}^4\text{F}_{3/2} \rightarrow {}^4\text{I}_{9/2}$. A manner to prove the antenna effect is to measure the lifetime of the excited states of the chromophore in presence and in absence of the acceptor, neodymium(III) in this case. It is therefore valid to propose that chromophores (**1**) and (**3**) behave as antennae.

Lifetimes for the mononuclear compound **4** and the dinuclear compound **10** are comparable to that reported for a tetranuclear system in solution⁵⁴ and a promising indication of an antenna effect through ligand and zinc coordination compound.

Fig. 9 shows a detailed view of the ${}^4\text{F}_{3/2}$ to ${}^4\text{I}_{9/2}$ luminescence band system and displays a comparison to the diffuse reflectance spectrum, showing the corresponding bands in absorption. The lower temperature spectra recorded at 80 K is well resolved and allows for a precise determination of maxima, as listed in Table 6. The spectra in Fig. 8 allow us to indicate the split of the ${}^4\text{I}_{9/2}$ level, information not usually available from such spectra,⁴⁸ and the resolution allows us to distinguish between the different types of structures described here.

The luminescence spectra of the dinuclear and trinuclear compounds are displayed in Fig. 10 and Fig. 11, respectively, where it can be observed that the luminescence maximum shows a red shift with the nuclearity of the compounds from the mononuclear (*ca.* 630 nm) to the dinuclear (*ca.* 640 nm) and to the trinuclear (*ca.* 700 nm) compounds.

Conclusions

A novel one-pot two-step synthetic route for the preparation of *d-f* heteronuclear coordination compounds is presented herein and it was possible to prepare mononuclear, dinuclear and trinuclear lanthanide-based complexes. The ligand is deprotonated when the inner compartment is occupied.

The luminescent properties varied upon modifying the chromophore employed, either just the organic ligand or a transition metal complex. From the three antennae employed in the present study H_2L (**1**), $[ZnL(OH_2)]$ (**2**) and $[NiL]$ (**3**), the first two sensitize neodymium(III) luminescence, even more the emission of the antenna was quenched; while the third one does not act as antenna.

Experimental

All reagents were purchased from Aldrich and used as received. The Infrared spectra were obtained using a Perkin-Elmer FTIR/FIR Spectrum 400 spectrometer. Elemental analyses were obtained in CHNS Perkin Elmer 2400 equipment; using cysteine for calibration. Effective magnetic moments of the compounds were determined in the solid state by the Gouy method, using a Johnson Matthey Type MSB model Auto magnetic balance. UV-Vis spectra were recorded on a Cary 6000i UV-Vis-NIR spectrophotometer. 1H and ^{13}C NMR spectra were recorded on a Varian Unity Inova spectrometer (400 and 75 MHz, respectively). Diffractograms were obtained using a Bruker D2-Phaser. Luminescence and Raman spectra were measured using an InVia spectrometer coupled to an imaging microscope (Leica) and argon ion lasers. The excitation wavelength used was 488 nm for all luminescence measurements and 785 for the Raman spectra. Temperature-dependent spectra were measured using a gas-flow microcryostat Linkam system. Electrical conductivity was measured in OAKTON PC2700 meter. Studies of the relaxation dynamics of the excited states of the ligand using Time-Correlated Single Photon counting (TCSPC) were carried out. The sample was excited by a picosecond pulse at 430 nm, provided by the second harmonic of a modelocked Ti:Sapph laser. The emitted light was then filtered by a monochromator and detected using a silicon avalanche photodiode (APD) synchronized with each repetition of the laser, one every 13 ns. By repeatedly counting the time between a synchronization signal and a triggering event of the APD, a histogram representing the decay of the PL was constructed. The power was kept at 100 μW and focused on a spot of *ca.* 300 μm diameter to avoid bleaching and other unwanted effects. The lifetime of the zinc(II) and nickel(II) chromophores, as well as the three neodymium(III) coordination compounds were obtained using a 400 nm femtosecond pulsed laser beam from a frequency

doubled Ti:Sapph multipass amplifier. The decay of the photoluminescence was recorded using a gated intensified CCD.

Computational details of H_2L

All the calculations were performed with the Gaussian 09 package (Gaussian Inc.)⁵⁵ using methods as they are implemented in the software. Initially, a ground-state geometry optimization was performed in the gas-phase on a single molecule starting from the crystal structure geometric parameters (bond lengths, angles and dihedral angles)⁵⁶ with the B3LYP exchange-correlation functional^{57,58} and the 6-311G(d,p) basis set. A frequency calculation was performed at the same level of theory on the obtained optimized structure to yield the calculated IR and Raman spectra presented with an arbitrary full-width-at-half-maximum (FWHM) of 4 cm⁻¹ for the calculated transitions. The absence of imaginary frequencies in the latter calculation confirms the global energy minimum nature of the calculated structure. Molecular orbitals were also calculated for this optimized structure and were visualized with the 5.08 release of the GaussView software (Gaussian Inc.)⁵⁵ with an isovalue of 0.02 atomic units.

Furthermore, excitation energies were evaluated for the discussed ligand by mean of the time-dependent density functional theory (TD-DFT)⁵⁵ with the aforementioned functional and basis set. The calculation was carried out in solution (methanol) with a polarizable continuum model (PCM)⁵⁹ using the optimized structure in this media with the same optimization method described earlier. The calculated absorption spectrum was then obtained by arbitrarily setting the full-width-at-half-maximum (FWHM) of the calculated transitions to 2200 cm⁻¹.

X-ray crystallography

Crystals of $[DyZn(O_2NO)_2(Cl)(L)(EtOH)] \cdot 3EtOH$ (**15a**), $[SmZn(O_2NO)_3(L)(OH_2)] \cdot EtOH$ (**16**) and $[TbZn_2(L)_2(Cl)_2(OH_2)](NO_3) \cdot EtOH$ (**23**) mounted on glass fibre were studied on an Oxford Diffraction Gemini "A" diffractometer with a CCD area detector ($\lambda_{MoK\alpha} = 0.71073 \text{ \AA}$, monochromator: graphite) source equipped with a sealed tube X-ray source at 130 K. Unit cell constants were determined with a set of 15/3 narrow frame/runs (1° in ω) scans. A data set consisted of 464, 288 and 302 frames of intensity data collected for (**15a**), (**16**) and (**23**)

respectively with a frame width of 1° in ω , a counting time of 12 s/frame, and a crystal-to-detector distance of 55.00 mm. The double pass method of scanning was used to exclude any noise. The collected frames were integrated by using an orientation matrix determined from the narrow frame scans.

CrysAlisPro and CrysAlis RED software packages were used for data collection and data integration.⁶⁰ Analysis of the integrated data did not reveal any decay. Final cell constants were determined by a global refinement of 3986, 3635 and 12922 reflections ($\theta < 29^\circ$) for **(15a)**, **(16)** and **(23)**, respectively. Collected data were corrected for absorbance by using Analytical numeric absorption correction using a multifaceted crystal model based on expressions upon the Laue symmetry using equivalent reflections.⁶¹ Structure solution and refinement were carried out with the program(s): SHELXS-2014; SHELXL-2014;⁶² for molecular graphics: Mercury program;⁶³ and the software used to prepare material for publication: WinGX.⁶⁴

Full-matrix least-squares refinement was carried out by minimizing $(Fo^2 - Fc^2)^2$, and using the SQUEEZE program.⁶⁵ All non-hydrogen atoms were refined anisotropically.

H atoms attached to O were located in a difference map and refined as riding on their parent atoms, with O—H = 0.82–0.86 Å and $U_{iso}(\text{H}) = 1.5U_{eq}(\text{O})$. H atoms attached to C atoms were placed in geometrically idealized positions and refined as riding on their parent atoms, with C—H = 0.95 – 0.99 Å with $U_{iso}(\text{H}) = 1.2U_{eq}(\text{C})$ for aromatic, methylene and methyne groups, and $U_{iso}(\text{H}) = 1.5 U_{eq}(\text{C})$ for methyl group. Crystal data and experimental details of the structures determination are listed in Table 2.

Crystallographic data have been deposited at the Cambridge Crystallographic Data Centre as supplementary material number CCDC 1409842-1409844. Copies of the data can be obtained free of charge on application to CCDC, 12 Union Road, Cambridge CB2 1EZ, UK. E-mail: deposit@ccdc.cam.ac.uk.

Synthesis of symmetrical Schiff base (antenna group)

N,N'-bis(3-hydroxyl salicylidene)benzene-1,2-diamine, (H_2L). A mixture of *o*-phenyldiamine (1.0814 g, 10 mmol) and 2,3-dihydroxybenzaldehyde (2.7624 g, 20 mmol) was refluxed in ethanol (120 mL) during 6 hours, then a red precipitate was formed. The product was isolated by filtration and washed with hot ethanol (3x10 mL) and finally dried under vacuum.

H_2L , **1**. The product was isolated as a red solid. Yield: 88% (3.0534 g). Anal. calcd. (found) for $C_{20}H_{16}N_2O_4$: %C 69.0 (68.9), %H: 4.6 (4.4), %N 8.0 (8.2). ^{13}C -RMN (400MHz, DMSO- d^6 , 298 K). δ (ppm): 118.8 (C-5), 119.2 (C-4), 119.6 (C-1), 120.0 (C-9), 122.8 (C-6), 127.8 (C-10), 142.2 (C-8), 145.7 (C-3), 149.5 (C-2), 164.8 (C-7). 1H -RMN (400 MHz, DMSO- d^6 , 298 K). δ (ppm): 6.77-6.81 (2H, t, $J=7.8$ Hz, H-5), 6.93-6.96 (2H, dd, $J=1.5, 7.8$ Hz, H-4), 7.10-7.13 (2H, dd, $J=1.5, 7.8$ Hz, H-6), 7.38-7.45 (4H, m, H-10, H-9), 8.88 (2H, s, H-7), 9.26 (2H, s, OH-3), 12.91 (2H, s, OH-2).

Synthesis of the antenna groups containing transition metal ions

$[Ni(L)]$, **2**. This compound was obtained by dissolving 0.3484 g (1mmol) of the ligand in hot ethanol; then an ethanolic solution containing 1 mmol of the transition metal ion was added. The reaction mixture was stirred for two hours at room temperature. The precipitate was filtered off, washed with hot ethanol (3x10 mL) and vacuum dried for 24 h.

The reaction of 1 mmol of $NiCl_2 \cdot 6H_2O$ or $Ni(NO_3) \cdot 6H_2O$ with 1 mmol of the ligand yielded $[Ni(L)]$, **2**. Yield 100% (0.4050 g). Anal. calcd. (found) for $C_{20}H_{14}N_2O_4Ni$, %C 59.3 (59.8), %H 3.5 (3.1), %N 6.9 (7.3). ^{13}C -RMN (400MHz, DMSO- d^6 , 298 K). δ (ppm): 115.4 (C-5), 115.7 (C-4), 116.4 (C-9), 119.3 (C-1), 123.4 (C-6), 127.7 (C-10), 142.2 (C-8), 148.2 (C-3), 154.6 (C-2), 156.7 (C-7). 1H -RMN (400 MHz, DMSO- d^6 , 298 K). δ (ppm): 6.52-6.55 (2H, t, $J=7.5$ Hz, H-5), 6.80-6.82 (2H, d, $J=7.0$ Hz, H-4), 7.08-7.10 (2H, dd, $J=1.5, 8.2$ Hz, H-6), 7.33-7.35 (2H, m, H-10), 8.13-8.18 (2H, m, H-9), 8.55 (2H, s, OH-3), 9.11 (2H, s, H-7).

The compound $[Zn(L)(OH_2)]$, **3** was similarly obtained using either $ZnCl_2$ or $Zn(NO_3) \cdot 6(H_2O)$. Yield 35% (0.1516 g). Anal. calcd. (found) for $C_{20}H_{16}N_2O_5Zn$, %C 56.3 (55.9), %H 3.4 (3.8), %N 6.9 (6.5). ^{13}C -RMN (400MHz, DMSO- d^6 , 298 K). δ (ppm): 112.9 (C-5), 114.0 (C-4), 116.6 (C-9), 117.4(C-1), 125.2 (C-6), 127.4 (C-10), 139.2(C-8), 149.6(C-3), 160.3 (C-2), 162.8 (C-7). 1H -RMN (400 MHz, DMSO- d^6 , 298 K). δ (ppm): 6.40-6.44 (2H, t, $J=7.5$ Hz, H-5), 6.80-6.82 (2H, dd, $J=1.6, 7.3$ Hz, H-4), 6.93-6.95 (2H, dd, $J=1.6, 8.2$ Hz, H-6), 7.337-7.4 (2H, m, H-10), 87.91-7.95 (2H, m, H-9), 8.07 (2H, s, OH-3), 9.05 (2H, s, H-7). The compound precipitated after the addition of 50 mL of distilled ice-cold water.

Synthesis of the mononuclear compounds

$[\text{Ln}(\text{O}_2\text{NO})_3(\text{H}_2\text{L})] \cdot n(\text{H}_2\text{O})$, ($\text{Ln}^{\text{III}} = \text{Nd}$, **4**; **Sm**, **5**; **Eu**, **6**; **Gd**, **7**; **Tb**, **8** and **Dy**, **9**). These compounds were prepared using a similar method. A typical procedure is described for compound **4**. To a boiling ethanol solution of the ligand (0.3484 g, 1 mmol), a solution of $\text{Nd}(\text{NO}_3)_3 \cdot 6\text{H}_2\text{O}$ (0.4384 g, 1 mmol) in ethanol was slowly added. The resulting solution was stirred for 1 h at room temperature. The orange precipitate was collected, washed with hot ethanol and vacuum dried for 24 h. Yield: 73% (0.5141 g). Anal. calcd. (found) for $\text{C}_{20}\text{H}_{19}\text{N}_5\text{O}_{14.5}\text{Nd}$, %C 34.0 (34.2), %H 2.7 (2.5), %N 9.9 (9.5). Compound **5**. Yield: 67% (0.4708 g). Anal. calcd. (found) for $\text{C}_{20}\text{H}_{17}\text{N}_5\text{O}_{14}\text{Sm}$, %C 34.2 (33.9), %H 2.4 (2.6), %N 10.0 (10.0). Compound **6**. Yield: 69% (0.5008 g). Anal. calcd. (found) for $\text{C}_{20}\text{H}_{20}\text{N}_5\text{O}_{15}\text{Eu}$, %C 33.3 (33.4), %H 2.8 (2.5), %N 9.7 (9.2). Compound **7**. Yield: 73% (0.5302 g). Anal. calcd. (found) for $\text{C}_{20}\text{H}_{20}\text{N}_5\text{O}_{15}\text{Gd}$, %C 33.0 (33.4), %H 2.8 (2.6), %N 9.6 (9.4). Compound **8**. Yield 33% (0.2497 g). Anal. calcd. (found) for $\text{C}_{20}\text{H}_{23}\text{N}_5\text{O}_{16.5}\text{Tb}$, %C 31.8 (31.8), %H 3.1 (2.6), %N 9.3 (9.1). Compound **9**. Yield: 70% (0.5157 g). Anal. calcd. (found) for $\text{C}_{20}\text{H}_{21}\text{N}_5\text{O}_{15.5}\text{Dy}$, %C 32.4 (32.4), %H 2.9 (2.7), %N 9.4 (9.3). In all cases orange powders were obtained.

Synthesis of the dinuclear compounds

$[\text{LnZn}(\text{O}_2\text{NO})_2(\text{Cl})(\text{L})(\text{OH}_2)] \cdot n\text{H}_2\text{O}$, ($\text{Ln}^{\text{III}} = \text{Nd}$, **10**; **Sm**, **11**; **Eu**, **12**; **Gd**, **13**; **Tb**, **14** and **Dy**, **15**). These compounds were prepared using a similar method. A typical procedure is described for **10**. The ligand was dissolved in boiling ethanol, the flask was retired from the heating source, an ethanolic solution of ZnCl_2 (0.1363 g, 1 mmol) was slowly added, the solution was stirred for 10 minutes, then neodymium(III) nitrate (0.4384 g, 1 mmol) in ethanol (5 mL) was added. The solution was stirred for 1 h at room temperature. The precipitate was filtered off, washed with hot ethanol (3x10 mL) and vacuum dried for 24 h. Yield: 50% (0.3846 g). Anal. calcd. (found) for $\text{C}_{20}\text{H}_{20}\text{N}_4\text{O}_{13}\text{ClZnNd}$, %C 31.2 (31.1), %H 2.6 (2.2), %N 7.3 (7.8). Compound **11**. Yield: 54% (0.4007 g). Anal. calcd. (found) for $\text{C}_{20}\text{H}_{16}\text{N}_4\text{O}_{11}\text{ClZnSm}$, %C 32.5 (32.3), %H 2.2 (2.4), %N 7.6 (7.1). Compound **12**. Yield: 57% (0.4361 g). Anal. calcd. (found) for $\text{C}_{20}\text{H}_{18}\text{N}_4\text{O}_{12}\text{ClZnEu}$, %C 31.6 (31.4), %H 2.4 (2.5), %N 7.4 (7.7). Compound **13**. Yield: 60% (0.4809 g). Anal. calcd. (found) for $\text{C}_{20}\text{H}_{22}\text{N}_4\text{O}_{14}\text{ClZnGd}$, %C 30.0 (29.7), %H 2.8 (2.3), %N 7.0 (7.0). Compound **14**. Yield: 64% (0.5132 g). Anal. calcd. (found) for $\text{C}_{20}\text{H}_{22}\text{N}_4\text{O}_{14}\text{ClZnTb}$, %C

29.9 (29.5), %H 2.8 (2.3), %N 7.0 (7.0). Compound **15**. Yield: 65% (0.4862 g). Anal. calcd. (found) for $C_{20}H_{16}N_4O_{11}ClZnDy$, %C 32.0 (32.1), %H 2.1 (2.1), %N 7.5 (7.2). Yellow solids were obtained in all cases. Suitable crystals of $[DyZn(O_2NO)_2(Cl)(L)(EtOH)] \cdot 3(EtOH)$ (**15a**) used for the X-ray structure determination were obtained when the reaction was carried using a molar ratio ligand: zinc chloride: dysprosium nitrate, 2:2:1 in ethanol, after 5 days.

Compound **16**. Single crystals of $[SmZn(O_2NO)_3(L)(OH_2)] \cdot EtOH$ were utilized for the X-ray structure determination were obtained when the reaction was carried using a molar ratio ligand: zinc nitrate: samarium nitrate, 2:2:1 in ethanol, after 5 days.

Synthesis of the trinuclear compounds

$[LnNi_2(L)_2(Cl)]Cl(NO_3) \cdot nH_2O$, ($Ln^{III} = Nd, 17; Sm, 18; Eu, 19; Gd, 20; Tb, 21$ and $Dy, 22$).

All the complexes were synthesized using a similar procedure. A typical procedure is described for compound **17**. The Schiff base (0.3484 g, 1 mmol) was dissolved in hot ethanol, the flask was removed from the heating mantle, a solution of nickel(II) chloride (0.2377g, 1 mmol) in ethanol was added (5 mL), and it was stirred for 10 minutes, then 5 mL of an ethanolic solution containing $Nd(NO_3)_3 \cdot 6H_2O$ (0.2192 g, 0.5 mmol) was added; the resulting solution was stirred for 1 h. The precipitate was isolated by filtration, washed with hot ethanol (3x10 mL) and vacuum dried for 24 hours. Compound **17** Yield 87% (0.5019 g). Anal. Calcd. (found) for $C_{40}H_{36}N_5O_{15}Cl_2NdNi_2$ %C 41.6 (41.4) %H 2.7 (3.1) %N 6.0 (6.0). Compound **18** Yield 89% (0.5248 g). Anal. Calcd. (found) for $C_{40}H_{38}N_5O_{16}Cl_2Ni_2Sm$, %C 40.6 (40.2), %H 3.2 (2.6), %N 5.9 (6.4). Compound **19**. Yield 82% (0.5012 g). Anal. Calcd. (found) for $C_{40}H_{34}N_5O_{14}Cl_2Ni_2Eu$, %C 41.8 (41.5), %H 3.0 (2.6), %N 6.1 (6.4). Compound **20**. Yield 87% (g). Anal. Calcd. (found) for $C_{40}H_{32}N_5O_{13}Cl_2Ni_2Gd$, %C 42.4 (42.3), %H 2.8(2.8), %N 6.3 (6.2). Compound **21**. Yield 94% (0.5238 g). Anal. Calcd. (found) for $C_{40}H_{30}N_5O_{12}Cl_2Ni_2Tb$, %C 42.9 (43.1), %H 2.7 (2.7), %N 6.3 (6.5). Compound **22**. Yield 88% (0.4957 g). Anal. Calcd. (found) for $C_{40}H_{30}N_5O_{12}Cl_2Ni_2Dy$, %C 42.8 (42.7), %H 2.7 (2.5), %N 6.2 (6.3).

$[TbZn_2(L)_2(Cl)_2(OH_2)](NO_3) \cdot EtOH$, (**23**). It was synthesised as previously described, using $ZnCl_2$ instead of $NiCl_2 \cdot 6H_2O$.

Acknowledgements

D. Olea-Román thanks CONACyT for the student fellowship 234136. Financial support is acknowledged from DGAPA-UNAM Projects IN222513, and CONACyT 178851 and DGCI-UNAM for travel (to Montreal) and living expenses (Mexico City) support. We are grateful for research grants and fellowships from the Natural Sciences and Engineering Research Council of Canada. We also thank J. Durán-Hernández, R. Ramírez-Trejo, P. Fierro-Ramírez, M. Gutiérrez-Franco, N. López-Balbiux, V. Lemus-Neri, M. Monroy-Barreto and A. Tejeda-Cruz for technical support.

References

- 1 K. B. Yatsimirskii, N. K. Davidenko, *Coord. Chem. Rev.*, 1979, **27**, 223.
- 2 J. Georges, *Analyst*, 1993, **118**, 1481.
- 3 G. A. Crosby, R. E. Whan, J. J. Freeman, *J. Phys. Chem.*, 1962, **66**, 2493.
- 4 J.-C. G. Bünzli, *Coord. Chem. Rev.*, 2015, **293-294**, 19.
- 5 W.-J. Chai, W.-X. Li, X.-J. Sun, T. Ren, X.-Y. Shi, *J. Lumin.*, 2011, **131**, 225.
- 6 J.-C. G. Bünzli, C. Piguet, *Chem. Soc. Rev.*, 2005, **34**, 1048.
- 7 G. R. Choppin, D. R. Peterman *Coord. Chem. Rev.*, 1998, **174**, 283.
- 8 H. Xiao, M. Chen, C. Mei, H. Yin, X. Zhang, X. Cao, *Spectrochim. Acta, Part A*, 2011, **84**, 238.
- 9 S. Biju, M. L. P. Reddy, A. H. Cowley, K. V. Vasudevan, *J. Mater. Chem.*, 2009, **19**, 5179.
- 10 L.-N. Sun, H.-J. Zhang, J.-B. Yu, Q.-G. Meng, F.-Y. Liu, Ch.-Y. Peng, *J. Photochem. Photobiol., A*, 2008, **193** 153.
- 11 A. D'Aléo, F. Pointillart, L. Ouahab, C. Andraud, O. Maury, *Coord. Chem. Rev.*, 2012, **256**, 1604.
- 12 H. He, *Coord. Chem. Rev.*, 2014, **87**, 273.
- 13 H. Wei, G. Yu, Z. Zhao, Z. Liu, Z. Bian, Ch. Huang, *Dalton Trans.*, 2013, **42**, 8951.
- 14 Y. Zhong, L. Si, H. He, A. G. Sykes, *Dalton Trans.*, 2011, **40**, 11389.
- 15 G. Chen, H. Ågren, T. Y. Ohulchanskyy, P. N. Prasad, *Chem. Soc. Rev.*, 2015, **44**, 1680.
- 16 A. Foucault-Collet, K. A. Gogick, K. A. White, S. Villette, A. Pallier, G. Collet, C. Kieda, T. Li, S. J. Geib, N. L. Rosi, S. Petoud, *PNAS*, 2013, **110**, 17199.

- 17 R. Naccache, E. Martín-Rodríguez, N. Bogdan, F. Sanz-Rodríguez, M. d. C. Iglesias-de-la-Cruz, A. Juarranz-de-la-Fuente, F. Vetrone, D. Jaque, J. García-Solé, J. A. Capobianco, *Cancers*, 2012, **4**, 1067.
- 18 C. D. S. Brites, P. P. Lima, N. J. O. Silva, A. Millán, V. S. Amaral, F. Palacio, L. D. Carlos, *New J. Chem.*, 2011, **35**, 1177.
- 19 J.-C. G. Bünzli, *Acc. Chem. Res.*, 2006, **39**, 53.
- 20 J.-C. G. Bünzli and S. V. Eliseeva, "Basics of Lanthanide Photophysics", in *Lanthanide Luminescence: Photophysical, Analytical and Biological Aspects*, P. Haninen and H. Härmä (Eds.), Springer Ser. Fluoresc. (2010).
- 21 M. D. Ward, *Coord. Chem. Rev.*, 2010, **254**, 2634.
- 22 M. Eddaoudi, D.B. Moler, H. Li, B. Chen, T.M. Reineke, M. O'Keeffe, O.M. Yaghi, *Acc. Chem. Res.*, 2001, **34**, 319.
- 23 C. Piguet, J.-C.G. Bünzli, *Chem. Soc. Rev.*, 1999, **28**, 347.
- 247 P. Zanello, S. Tamburini, P.A. Vigato, G.A. Mazzocchin, *Coord. Chem. Rev.*, 1987, **77**, 165.
- 25 M. Albrecht, O. Osetska, J. Klankermayer, R. Fröhlich, F. Gumy, J.-C. G. Bünzli, *Chem. Commun.*, 2007, 1834.
- 26 B.L. An, M.L. Gong, *J. Fluoresc.*, 2005, **15**, 613.
- 27 P. Xi, X.H. Gu, *Spectrochim. Acta, Part A*, 2007, **66**, 667.
- 28 Y.G. Lv, J.C. Zhang, W.L. Cao, Y.L. Fua, *Spectrochim. Acta, Part A*, 2009, **72** 22.
- 29 X.Y. Liu, Y.L. Hu, B.Y. Wang, Z.X. Su, *Synth. Met.*, 2009, **159**, 1557.
- 30 X.Q. Song, J.R. Zheng, *Spectrochim. Acta, Part A*, 2008, **69**, 49.
- 31 X. Yang, A. Liao, J. M. Stanley, R. A. Jones, B. J. Holliday, *Polyhedron*, 2013, **52**, 165.
- 32 H. Wang, B. Zhang, Z.-H. Ni, X. Li, L. Tian, J. Jiang, *Inorg. Chem.*, 2009, **48**, 5946.
- 33 T. D. Pasatiou, C. Toseanu, A. M. Madalan, B. Jurca, C. Duhayon, J. P. Sutter, M. Andruh, *Inorg. Chem.*, 2011, **50**, 5879.
- 34 R. D. Archer, H. Chen, *Inorg. Chem.*, 1998, **37**, 2089.
- 35 V. Vicinelli, P. Ceroni, M. Maestri, V. Balzani, M. Gorka and F. Vögtle, *J. Am. Chem. Soc.*, 2002, **124**, 6461.
- 36 D. Nandan Kumar, B.S. Garg, *Spectrochim. Acta, Part A*, 2006, **64**, 141.
- 37 Q. Wang, X.-H. Yan, W.-S. Liu, M.-Y. Tan, Y. Tang, *J. Fluoresc.*, 2010, **20**, 493.

- 38 Z.-Z. Yan, Y. Tang, W.-S. Liu, M.-Y. Tan, *J. Lumin.*, 2008, **128**, 1394.
- 39 P. Chen, H. Chen, P. Yan, Y. Wang, G. Li, *CrystEngComm.*, 2011, **13**, 6237.
- 40 J. Wang., Y. Wang, X.-D. Zhang, Z.-H. Zhang, Y. Zhang, L. Ping K., H. Li, *J. Coord. Chem.*, 2005, **58**, 921.
- 41 J. Wang, X. Zh. Liu, Zh. H. Zhang, X. D. Zhang, G. R. Gao, Y. M. Kong, and Y. Li, *J. Struct. Chem.*, 2006, **47**, 906.
- 42 T. D. Pasatou, C. Tiseanu, A. M. Madalan, B. Jurca, C. Duhayon, J. P. Sutter, M. Andruh, *Inorg. Chem.*, 2011, **50**, 5879.
- 43 A. W. Addison, T. N. Rao, J. Reedijk, J. Rijn, G. C. Verschoor, *J. Chem. Soc., Dalton Trans.*, 1984, 1349.
- 44 D. N. Kumar, B.S. Garg, *Spectrochim. Acta, Part A*, 2006, **64**, 141.
- 45 D. V. R. Murthy, T. Sasikala, B. Jamalaiah, A. Mohan-Babu, J. Suresh-Kumar, M. Jayasimhadri, L. Rama-Moorthy, *Opt. Commun.*, 2011, **284**, 603.
- 46 G. Oczko, J. Legendziewicz, V. Trush, V. Amirkhanov, *New J. Chem.*, 2003, **27**, 948.
- 47 H. Jung, S. K. Yoon, J. G. Kim, J.-G. Kang, *Bull. Korean Chem. Soc.*, 1992, **13**, 650.
- 48 SW.-K. Wong, X. Yang, R. A. Jones, J. H. Rivers, V. Lynch, W.-K. Lo, D. Xiao, M. M. Oye, A. L. Holmes, *Inorg. Chem.*, 2006, **45**, 4340.
- 49 T. Brunold, H. U. Güdel, in *Inorganic Electronic Structure and Spectroscopy*, E. I. Solomon, A. B. P Lever, Eds. John Wiley & Sons, Inc.: New York, 1999; Vol. I, p. 259.
- 50 O. V. Kotova, S. V. Eliseeva, A. S. Averjushkin, A. G. Vitukhnovskii, L. S. Lepnev, A. A. Vaschenko, N. P. Kuzmina, A. Yu. Rogachev, *Russ. Chem. Bull., Int. Ed.*, 2008, **57**, 1880.
- 51 L. Armelao, S. Quici, F. Barigelletti, G. Accorsi, G. Bottaro, M. Cavazzini, E. Tondello, *Coord. Chem. Rev.*, 2010, **25**, 487.
- 52 C. Galaup, J. Azéma, P. Tisnès, C. Picard, *Helv. Chim. Acta*, 2002, **85**, 1613.
- 53 C. Huang, Z. Bian, in "Rare Earth Coordination Chemistry: Fundamentals and Applications", C. Huang, ed. John Wiley & Sons, Singapore, 2010, p. 7.
- 54 Z. Zhang, W. Feng, P. Su, L. Liu, X. Lü, W.-K. Wong, R. A. Jones, D. Fan, *Inorg. Chem. Commun.*, 2014, **48**, 48.
- 55 Gaussian 09, Revision D.01, M. J. Frisch, G. W. Trucks, H. B. Schlegel, G. E. Scuseria, M. A. Robb, J. R. Cheeseman, G. Scalmani, V. Barone, B. Mennucci, G. A. Petersson, H. Nakatsuji,

- M. Caricato, X. Li, H. P. Hratchian, A. F. Izmaylov, J. Bloino, G. Zheng, J. L. Sonnenberg, M. Hada, M. Ehara, K. Toyota, R. Fukuda, J. Hasegawa, M. Ishida, T. Nakajima, Y. Honda, O. Kitao, H. Nakai, T. Vreven, J. A. Montgomery, Jr., J. E. Peralta, F. Ogliaro, M. Bearpark, J. J. Heyd, E. Brothers, K. N. Kudin, V. N. Staroverov, R. Kobayashi, J. Normand, K. Raghavachari, A. Rendell, J. C. Burant, S. S. Iyengar, J. Tomasi, M. Cossi, N. Rega, J. M. Millam, M. Klene, J. E. Knox, J. B. Cross, V. Bakken, C. Adamo, J. Jaramillo, R. Gomperts, R. E. Stratmann, O. Yazyev, A. J. Austin, R. Cammi, C. Pomelli, J. W. Ochterski, R. L. Martin, K. Morokuma, V. G. Zakrzewski, G. A. Voth, P. Salvador, J. J. Dannenberg, S. Dapprich, A. D. Daniels, Ö. Farkas, J. B. Foresman, J. V. Ortiz, J. Cioslowski, and D. J. Fox, Gaussian, Inc., Wallingford CT, 2009.
- 56 M. J. Rodriguez-Douton, M. I. Fernandez, A. M. Gonzalez-Noya, M. Maneiro, R. Pedrido, M. J. Romero, *Synth. React. Inorg., Met.-Org., Nano-Met.Chem.*, 2006, **36**, 655.
- 57 A. D. Becke, *J. Chem. Phys.*, 1993, **98**, 5648.
- 58 J. Tirado-Rives, W. L. Jorgensen, *J. Chem. Theory Comput.*, 2008, **4**, 297.
- 59 J. Tomasi, B. Mennucci, R. Cammi, *Chem. Rev.*, 2005, **105**, 2999.
- 60 Agilent (2013). *CrysAlis PRO* and *CrysAlis RED*. Agilent Technologies, Yarnton, England.
- 61 R. C. Clark, J. S. Reid, *Acta Crystallogr. A*, 1995, **51**, 887.
- 62 G. M. Sheldrick, *Acta Crystallogr. A*, 2008, **64**, 112.
- 63 C. F. Macrae, P. R. Edgington, P. McCabe, E. Pidcock, G. P. Shields, R. Taylor, Towler and van der Streek, *J. Appl. Crystallogr.*, 2006, **39**, 453.
- 64 L. J. Farrugia, *J. Appl. Crystallogr.*, 1999, **32**, 837.
- 65 A. L. Spek, *J. Appl. Crystallogr.*, 2003, **36**, 7.

Table 1 Selected IR and Raman Vibrations and Effective Magnetic Moments.

Compound	cm ⁻¹					B. M.
	$\nu_{\text{N-C-H}}$ (IR)	$\nu_{\text{C-O}}$ (IR)	$\nu_{\text{C-O}}$ (Raman)	$\nu_{\text{C=N}}$ (IR)	$\nu_{\text{C=N}}$ (Raman)	μ_{eff}
H ₂ L (1)	3053	1272	1352	1611	1582	0
[Nd(O ₂ NO) ₃ (H ₂ L)]·1.5H ₂ O (4)	3061	1262	x	1618	x	3.25
[Sm(O ₂ NO) ₃ (H ₂ L)]·H ₂ O (5)	3062	1261	1257	1616	1594	1.69
[Eu(O ₂ NO) ₃ (H ₂ L)]·2H ₂ O (6)	3057	1263	1259	1617	1594	3.46
[Gd(O ₂ NO) ₃ (H ₂ L)]·2H ₂ O (7)	3060	1261	1265	1617	1592	8.24
[Tb(O ₂ NO) ₃ (H ₂ L)]·3.5H ₂ O (8)	3054	1259	1265	1616	1591	9.11
[Dy(O ₂ NO) ₃ (H ₂ L)]·2.5H ₂ O (9)	3056	1259	1264	1616	1592	10.46
[Zn(L)(OH ₂)] (3)	3060	1266	1278	1612	1619	0
[NdZn(O ₂ NO) ₂ (Cl)(L)(OH ₂)]·2H ₂ O (10)	3063	1249	x	1611	x	3.60
[SmZn(O ₂ NO) ₂ (Cl)(L)(OH ₂)] (11)	3062	1247	1240	1613	1615	1.45
[EuZn(O ₂ NO) ₂ (Cl)(L)(OH ₂)]·H ₂ O (12)	3064	1249	1242	1611	1612	3.32
[GdZn(O ₂ NO) ₂ (Cl)(L)(OH ₂)]·3H ₂ O (13)	3063	1249	1240	1611	1615	7.94
[TbZn(O ₂ NO) ₂ (Cl)(L)(OH ₂)]·3H ₂ O (14)	3063	1251	1192	1610	1613	9.46
[DyZn(O ₂ NO) ₂ (Cl)(L)(OH ₂)] (15)	3062	1247	1191	1611	1613	10.19
[Ni(L)] (2)	3054	1259	1198	1612	1595	0
[NdNi ₂ (L) ₂ (Cl)]Cl(NO ₃)·4H ₂ O (17)	3058	1255	1203	1607	1596	3.77
[SmNi ₂ (L) ₂ (Cl)]Cl(NO ₃)·4H ₂ O (18)	---	1256	1202	1607	1596	1.69
[EuNi ₂ (L) ₂ (Cl)]Cl(NO ₃)·3H ₂ O (19)	---	1259	1202	1607	1596	3.32
[GdNi ₂ (L) ₂ (Cl)]Cl(NO ₃)·2H ₂ O (20)	---	1258	1201	1606	1596	8.27
[TbNi ₂ (L) ₂ (Cl)]Cl(NO ₃)·H ₂ O (21)	---	1258	---	1606	---	9.45
[DyNi ₂ (L) ₂ (Cl)]Cl(NO ₃)·H ₂ O (22)	---	1259	1201	1606	1595	10.29

^xRaman signal masked by luminescence

Table 2 Crystal Data and Structure Refinement for Compounds (15a), (16) and (23).

	(15a)	(16)	(23)
Empirical formula	C ₂₈ H ₃₈ Cl Dy N ₄ O ₁₄ Zn	C ₂₂ H ₂₂ N ₅ O ₁₅ Sm Zn	C ₄₄ H ₄₁ Cl ₂ N ₅ O ₁₄ Tb Zn ₂
Formula weight	917.94	812.16	1224.38
Temp. (K)	130(2)	130(2)	130(2)
Wavelength (Å)	0.71073	0.71073	0.71073
Crystal system	Triclinic	Triclinic	Monoclinic
Space group	P -1	P -1	C 2/c
<i>a</i> (Å)	11.4819(9)	9.7146(14)	24.7686(11)
<i>b</i> (Å)	13.1424(9)	12.1476(13)	12.1074(3)
<i>c</i> (Å)	13.8087(10)	12.9509(6)	21.6863(10)
α (°)	71.062(6)	83.090(7)	90
β (°)	77.213(6)	71.598(10)	123.588(6)
γ (°)	80.759(6)	87.232(10)	90
Volume (Å ³)	1913.1(3)	1439.6(3)	5417.5(5)
<i>Z</i>	2	2	4
<i>D</i> _{calc} (Mg/m ³)	1.593	1.874	1.501
Absorption coefficient (mm ⁻¹)	2.699	2.933	2.330
<i>F</i> (000)	918	802	2444
Crystal size (mm ³)	0.450 x 0.210 x 0.080	0.600 x 0.100 x 0.080	0.510 x 0.290 x 0.240
Theta range for data collection (°)	3.370 to 29.491	3.505 to 29.447	3.399 to 29.534
Index ranges	-14<= <i>h</i> <=12, -16<= <i>k</i> <=16, - 19<= <i>l</i> <=15	-12<= <i>h</i> <=10, -16<= <i>k</i> <=16, - 17<= <i>l</i> <=16	-30<= <i>h</i> <=34, -12<= <i>k</i> <=15, - 29<= <i>l</i> <=28
Reflections collected	15475	11225	23768
Independent reflections	8954 [R(int) = 0.0542]	6696 [R(int) = 0.0335]	6710 [R(int) = 0.0229]
Completeness to theta = 25.242°	99.7 %	99.7 %	99.7 %
Refinement method	Full-matrix least-squares on F ²	Full-matrix least-squares on F ²	Full-matrix least-squares on F ²
Data / restraints / parameters	8954 / 51 / 448	6696 / 53 / 419	6710 / 24 / 318
Goodness-of-fit on F ²	1.065	1.061	1.087
Final R indices [I>2sigma(I)]	R1 = 0.0591, wR2 = 0.1334	R1 = 0.0352, wR2 = 0.0711	R1 = 0.0387, wR2 = 0.1115
R indices (all data)	R1 = 0.0786, wR2 = 0.1434	R1 = 0.0465, wR2 = 0.0772	R1 = 0.0444, wR2 = 0.1159
Largest diff. peak and hole (e.Å ⁻³)	3.671 and -2.196	0.932 and -1.057	2.661 and -1.062

Table 3 Selected Bond lengths (Å) and Angles (deg) for Compound **15a**.

Zn(1)-Cl(1)	2.2680(17)	O(8)-Zn(1)-Cl(1)	105.68(13)
N(10)-Zn(1)	2.053(5)	O(19)-Zn(1)-Cl(1)	105.82(14)
N(17)-Zn(1)	2.042(5)	N(17)-Zn(1)-Cl(1)	113.85(16)
O(8)-Zn(1)	2.017(4)	N(10)-Zn(1)-Cl(1)	113.84(14)
O(19)-Zn(1)	2.018(4)	O(8)-Dy(1)-O(05)	134.35(15)
Zn(1)-Dy(1)	3.5002(8)	O(8)-Dy(1)-O(07)	76.90(16)
O(19)-Dy(1)	2.288(4)	O(8)-Dy(1)-O(04)	145.93(18)
O(26)-Dy(1)	2.481(4)	O(07)-Dy(1)-O(04)	124.34(15)
O(01)-Dy(1)	2.501(5)	O(05)-Dy(1)-O(04)	53.20(16)
O(1)-Dy(1)	2.476(4)	O(8)-Dy(1)-O(1)	64.93(14)
O(02)-Dy(1)	2.482(4)	O(1)-Dy(1)-O(26)	163.21(14)
O(04)-Dy(1)	2.438(4)	O(8)-Dy(1)-O(02)	102.05(16)
O(05)-Dy(1)	2.412(5)	O(19)-Dy(1)-O(02)	76.25(16)
O(07)-Dy(1)	2.379(5)	O(07)-Dy(1)-O(02)	153.83(17)
O(8)-Dy(1)	2.285(4)	O(05)-Dy(1)-O(02)	120.84(16)
O(8)-Zn(1)-O(19)	74.87(17)	O(19)-Dy(1)-O(01)	103.33(15)
O(8)-Zn(1)-N(17)	140.1(2)	O(07)-Dy(1)-O(01)	147.95(15)
O(19)-Zn(1)-N(17)	88.84(18)	O(05)-Dy(1)-O(01)	118.56(17)
O(8)-Zn(1)-N(10)	88.4(2)	O(04)-Dy(1)-O(01)	74.18(16)
O(19)-Zn(1)-N(10)	139.8(2)	O(1)-Dy(1)-O(01)	69.17(14)
N(17)-Zn(1)-N(10)	81.0(2)	O(02)-Dy(1)-O(01)	50.80(14)

Table 4 Selected Bond lengths (Å) and Angles (deg) for Compound **16**.

N(10)-Zn(2)	2.028(3)	O(8)-Zn(2)-N(10)	92.13(12)
N(17)-Zn(2)	2.055(3)	O1WBb-Zn(2)-N(17)	116.52(19)
O(8)-Zn(2)	2.002(2)	O(19)-Zn(2)-N(17)	91.55(11)
O(19)-Zn(2)	1.978(3)	O(8)-Zn(2)-N(17)	151.42(12)
Zn(2)-O1WBb	1.970(6)	N(10)-Zn(2)-N(17)	80.70(12)
Zn(2)-O1WAa	2.124(6)	O(19)-Zn(2)-O1WAa	96.29(18)
Zn(2)-Sm(1)	3.5206(6)	O(8)-Zn(2)-O1WAa	109.82(17)
O(01)-Sm(1)	2.515(2)	N(10)-Zn(2)-O1WAa	115.60(19)
O(1)-Sm(1)	2.513(2)	N(17)-Zn(2)-O1WAa	98.14(18)
O(03)-Sm(1)	2.595(2)	O(8)-Sm(1)-O(19)	64.31(8)
O(04)-Sm(1)	2.513(3)	O(8)-Sm(1)-O(07)	74.03(9)
O(05)-Sm(1)	2.508(3)	O(19)-Sm(1)-O(07)	75.73(10)
O(07)-Sm(1)	2.505(3)	O(8)-Sm(1)-O(05)	79.20(8)
O(08)-Sm(1)	2.544(3)	O(19)-Sm(1)-O(05)	112.66(9)
O(8)-Sm(1)	2.515(2)	O(07)-Sm(1)-O(05)	144.63(8)
O(19)-Sm(1)	2.401(2)	O(8)-Sm(1)-O(1)	63.22(8)
O(26)-Sm(1)	2.523(2)	O(19)-Sm(1)-O(1)	123.74(8)
O1WBb-Zn(2)-O(19)	108.77(19)	O(07)-Sm(1)-O(1)	71.84(9)
O1WBb-Zn(2)-O(8)	92.01(18)	O(05)-Sm(1)-O(1)	75.66(8)
O(19)-Zn(2)-O(8)	79.88(10)	O(8)-Sm(1)-O(04)	85.20(10)
O1WBb-Zn(2)-N(10)	102.52(19)	O(19)-Sm(1)-O(04)	70.92(9)
O(19)-Zn(2)-N(10)	147.87(13)	O(07)-Sm(1)-O(04)	145.90(9)

Table 5 Selected Bond lengths (Å) and Angles (deg) for Compound (**23**).

N(1)-Zn(1)	2.043(3)	N(2)-Zn(1)-N(1)	80.57(13)
N(2)-Zn(1)	2.030(3)	O(2)-Zn(1)-Cl(1)	111.74(8)
O(2)-Zn(1)	2.007(2)	O(3)-Zn(1)-Cl(1)	109.05(8)
Cl(1)-Zn(1)	2.3064(10)	N(2)-Zn(1)-Cl(1)	102.63(9)
O(3)-Zn(1)	2.009(2)	N(1)-Zn(1)-Cl(1)	103.68(9)
Zn(1)-Tb(1)	3.4972(4)	O(2)#2-Tb(1)-O(4)	72.99(9)
O(1)-Tb(1)	2.486(3)	O(1)#2-Tb(1)-O(1)	78.36(13)
O(4)-Tb(1)	2.516(3)	O(3)-Tb(1)-O(1)#2	76.90(9)
O(3)-Tb(1)	2.353(2)	O(2)-Tb(1)-O(1)#2	78.11(9)
O(2)-Tb(1)	2.344(2)	O(3)#2-Tb(1)-O(1W)	76.09(6)
O(2)-Zn(1)-O(3)	78.35(10)	O(2)-Tb(1)-O(1)	63.86(8)
O(2)-Zn(1)-N(2)	145.63(11)	O(2)-Tb(1)-O(3)	65.37(8)
O(3)-Zn(1)-N(2)	90.94(11)	O(1W)-Tb(1)-O(4)	69.96(7)
O(2)-Zn(1)-N(1)	90.95(11)	O(1)-Tb(1)-O(4)#2	72.79(9)
O(3)-Zn(1)-N(1)	147.25(12)	O(2)-Tb(1)-O(4)#2	72.99(9)

Symmetry transformations used to generate equivalent atoms: #1 -x+1,-y,-z+2 #2 -x+1,y,-z+3/2

Table 6 Spectroscopic Results of Coordination Compounds of different nuclearity.

Compound	Absorption maxima (nm)	Luminescence maxima (nm)
H ₂ L (1)	285 (32262 M ⁻¹ cm ⁻¹) 334 (2469 M ⁻¹ cm ⁻¹) 468 (6259 M ⁻¹ cm ⁻¹), 450 ^a	625
[Eu(O ₂ NO) ₃ (H ₂ L)]·2H ₂ O (6)	512 ^a	691
[Gd(O ₂ NO) ₃ (H ₂ L)]·2H ₂ O (7)	511 ^a	638
[Tb(O ₂ NO) ₃ (H ₂ L)]·3.5H ₂ O (8)	505 ^a	649
[Zn(L)(OH ₂)] (3)	508 ^a	598
[EuZn(O ₂ NO) ₂ (Cl)(L)(OH ₂)]·H ₂ O (12)	429 ^a	680
[GdZn(O ₂ NO) ₂ (Cl)(L)(OH ₂)]·3H ₂ O (13)	433 ^a	634
[TbZn(O ₂ NO) ₂ (Cl)(L)(OH ₂)]·3H ₂ O (14)	426 ^a	642
[Ni(L)] (2)	478 ^a	716
[EuNi ₂ (L) ₂ (Cl)]Cl(NO ₃)·3H ₂ O (19)	444 ^a	713
[GdNi ₂ (L) ₂ (Cl)]Cl(NO ₃)·2H ₂ O (20)	451 ^a	704
[TbNi ₂ (L) ₂ (Cl)]Cl(NO ₃)·H ₂ O (21)	443 ^a	704, 756 (sh)
	434 ^a	
	678 ^{a,b}	872, 880, 903, 909 ^f
[Nd(O ₂ NO) ₃ (H ₂ L)]·1.5H ₂ O (4)	735 ^{a,c}	1041, 1051, 1070 ^g
	796 ^{a,d}	
	868 ^{a,e}	
	517 ^a	
[Sm(O ₂ NO) ₃ (H ₂ L)]·H ₂ O (5)	946 ^{a,h}	630
	1084 ^{a,i}	
	505 ^a	
	761 ^{a,j}	
[Dy(O ₂ NO) ₃ (H ₂ L)]·2.5H ₂ O (9)	810 ^{a,k}	649
	902 ^{a,l}	
	1091 ^{a,m}	
	434 ^a	
	577 ^{a,n}	
[NdZn(O ₂ NO) ₂ (Cl)(L)(OH ₂)]·2H ₂ O (10)	738 ^{a,c}	873, 879, 906, 913 ^f
	797 ^{a,d}	1058 ^g
	868 ^{a,e}	
	432 ^a	
[SmZn(O ₂ NO) ₂ (Cl)(L)(OH ₂)] (11)	946 ^{a,h}	628
	1088 ^{a,i}	
	431 ^a	
	805 ^{a,k}	
[DyZn(O ₂ NO) ₂ (Cl)(L)(OH ₂)] (15)	904 ^{a,l}	636
	1105 ^{a,m}	
[NdNi ₂ (L) ₂ (Cl)]Cl(NO ₃)·4H ₂ O (17)	704, 766 ^a	700 879 ^f
	439 ^a	
[SmNi ₂ (L) ₂ (Cl)]Cl(NO ₃)·4H ₂ O (18)	947 ^{a,h}	705
	1087 ^{a,i}	
	451 ^a	
	751 ^{a,j}	
[DyNi ₂ (L) ₂ (Cl)]Cl(NO ₃)·H ₂ O (22)	804 ^{a,k}	705
	904 ^{a,l}	
	1101 ^{a,m}	

^a Diffuse reflectance

^b ${}^4I_{9/2} \rightarrow {}^4F_{9/2}$ (Nd^{3+} absorption)⁴⁵

^c ${}^4I_{9/2} \rightarrow {}^4F_{7/2} + {}^4S_{3/2}$ (Nd^{3+} absorption)⁴⁵

^d ${}^4I_{9/2} \rightarrow {}^4F_{5/2} + {}^2H_{9/2}$ (Nd^{3+} absorption)⁴⁵

^e ${}^4I_{9/2} \rightarrow {}^4F_{3/2}$ (Nd^{3+} absorption)⁴⁵

^f ${}^4F_{3/2} \rightarrow {}^4I_{9/2}$ (Nd^{III} emission)⁴⁸

^g ${}^4F_{3/2} \rightarrow {}^4I_{11/2}$ (Nd^{III} emission)⁴⁸

^h ${}^6H_{5/2} \rightarrow {}^6F_{11/2}$ (Sm^{III} absorption)⁴⁶

ⁱ ${}^6H_{5/2} \rightarrow {}^6F_{9/2}$ (Sm^{III} absorption)⁴⁶

^j ${}^6H_{15/2} \rightarrow {}^6F_{3/2}$ (Dy^{III} absorption)⁴⁷

^k ${}^6H_{15/2} \rightarrow {}^6F_{5/2}$ (Dy^{III} absorption)⁴⁷

^l ${}^6H_{15/2} \rightarrow {}^6H_{5/2} + {}^6F_{7/2}$ (Dy^{III} absorption)⁴⁷

^m ${}^6H_{15/2} \rightarrow {}^6F_{9/2} + {}^6H_{7/2}$ (Dy^{III} absorption)⁴⁷

ⁿ ${}^4I_{9/2} \rightarrow {}^4G_{5/2}$ (Nd^{III} absorption)⁴⁵

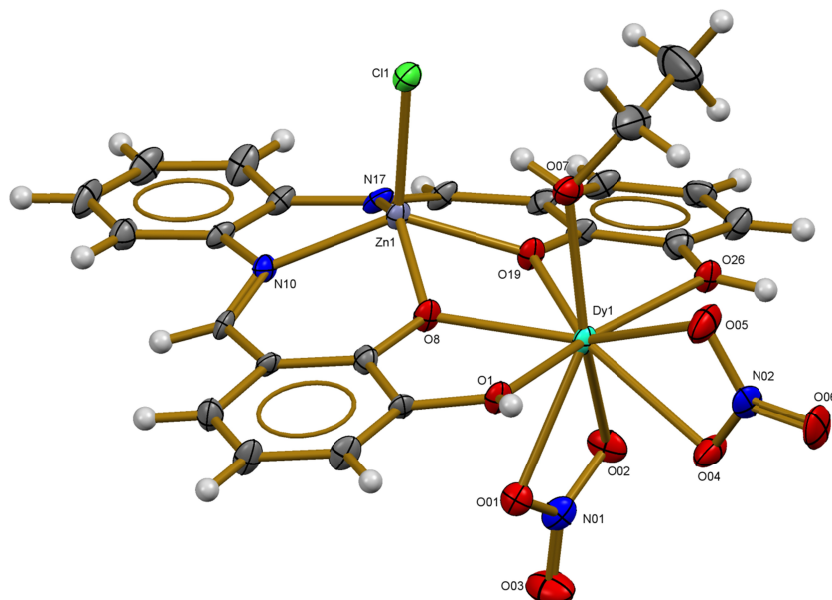


Fig. 1 ORTEP picture of the molecular structure of dinuclear $[DyZn(O_2NO)_2(Cl)(L)(EtOH)] \cdot 3(EtOH)$ **15a** with the thermal ellipsoids drawn at 50% of probability. The crystallisation ethanol molecule and the nitrate anion were omitted for clarity

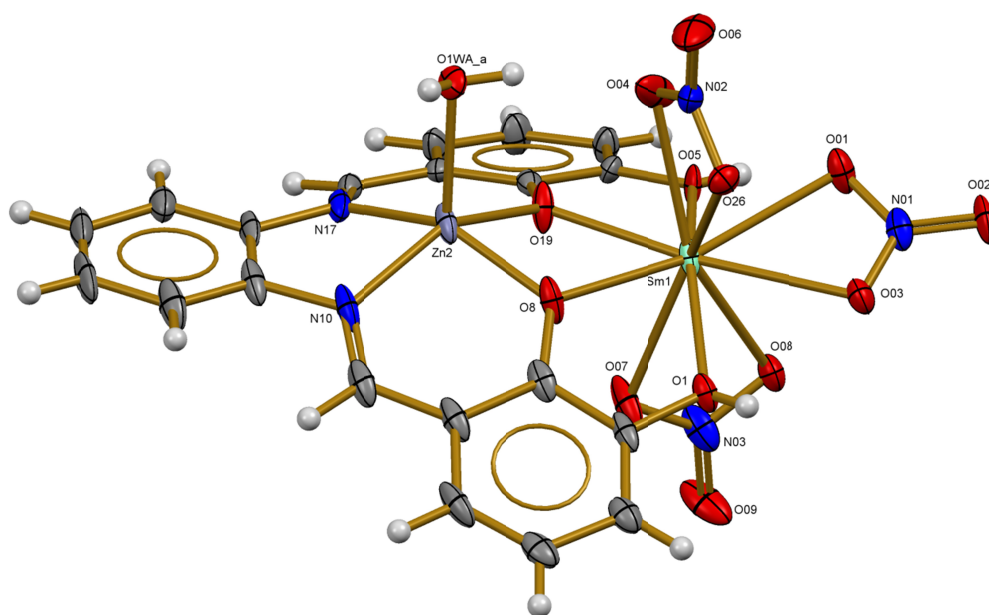


Fig. 2 ORTEP picture of the molecular structure of dinuclear $[SmZn(O_2NO)_3(L)(OH_2)] \cdot EtOH$ **16** with the thermal ellipsoids drawn at the 50% of probability. The ethanol solvent molecule was omitted for clarity

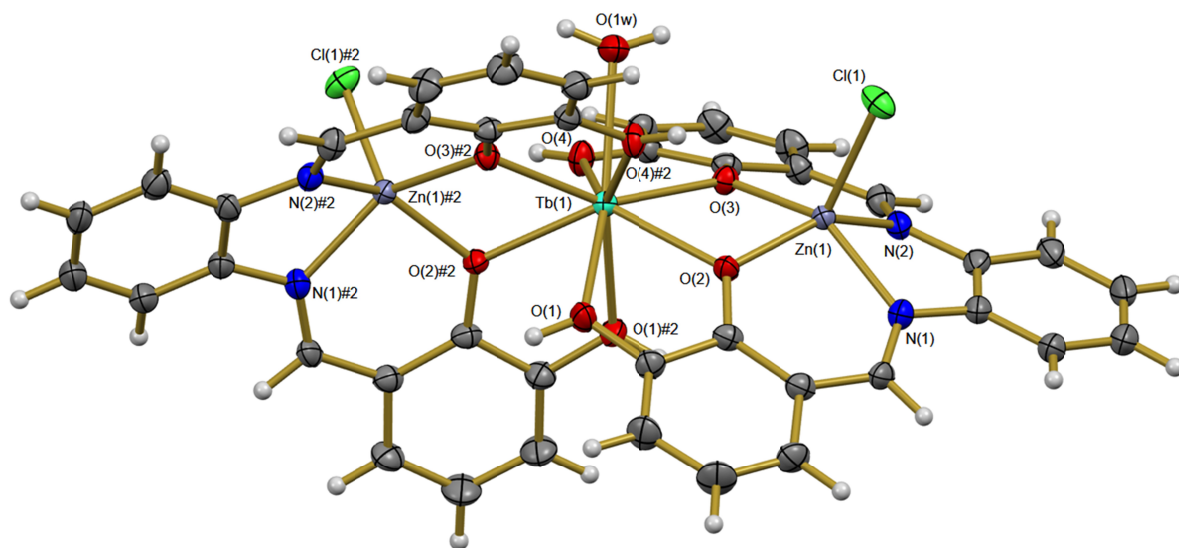


Fig. 3 ORTEP picture of the molecular structure of dinuclear $[TbZn_2(L)_2(Cl)_2(OH_2)](NO_3) \cdot EtOH$ (**23**) with the thermal ellipsoids drawn at the 50% of probability. The ethanol solvent molecules were omitted for clarity. Symmetry transformations used to generate equivalent atoms: #1 $-x+1, -y, -z+2$ #2 $-x+1, y, -z+3/2$

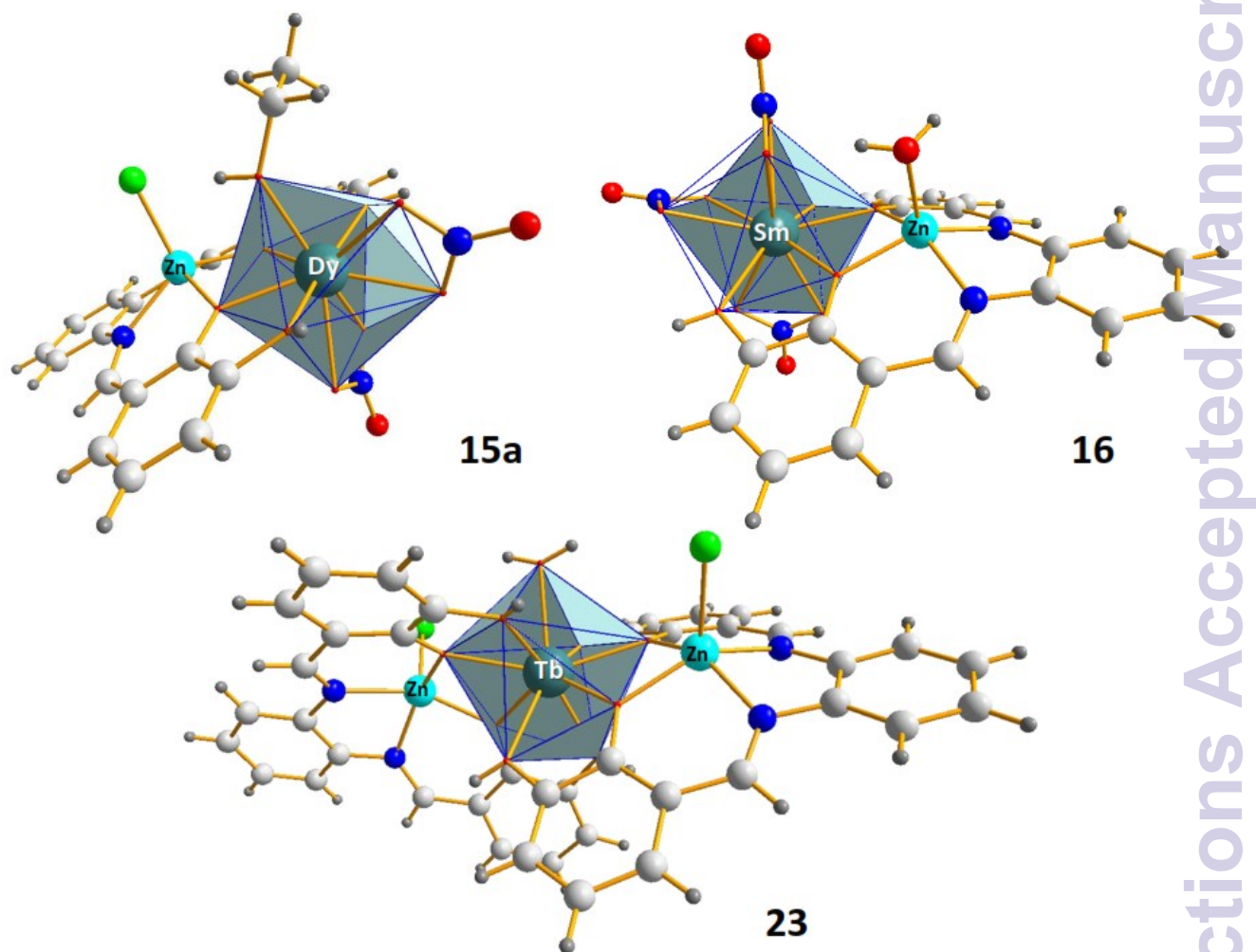


Fig. 4 Geometry of lanthanide ions of compounds **15a**, **16** and **23** displayed as polyhedra

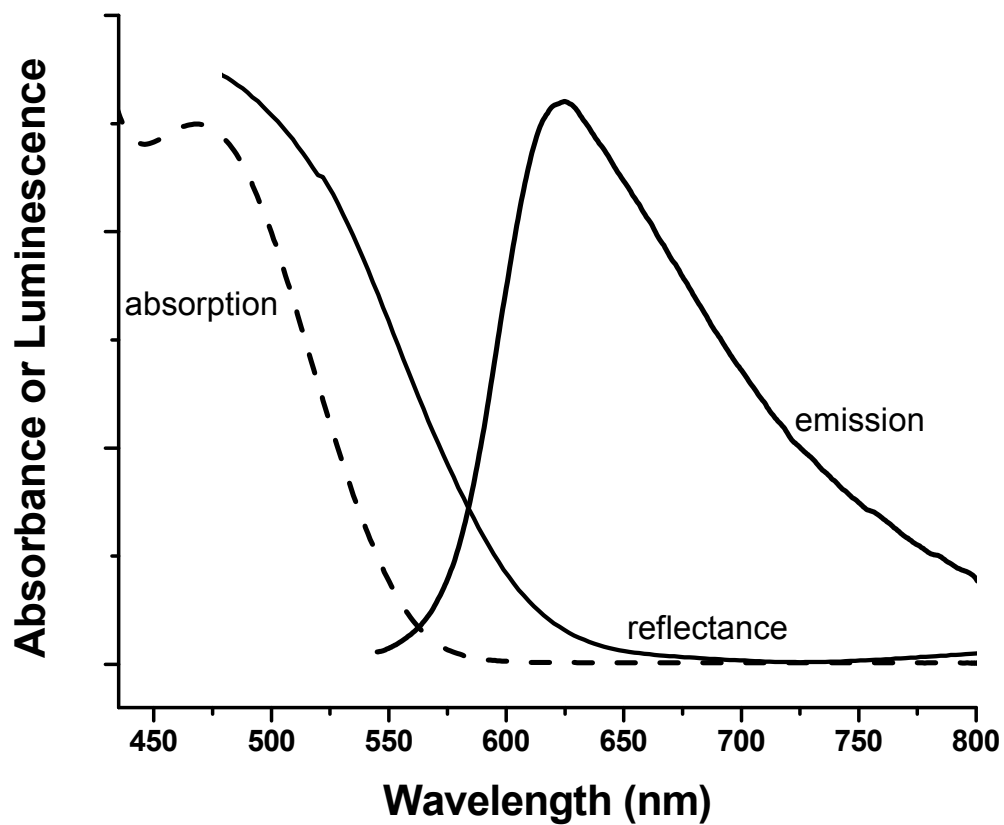


Fig. 5 Absorption in MeOH, diffuse reflectance and luminescence spectra of the ligand (H_2L).

λ_{ex} 488 nm

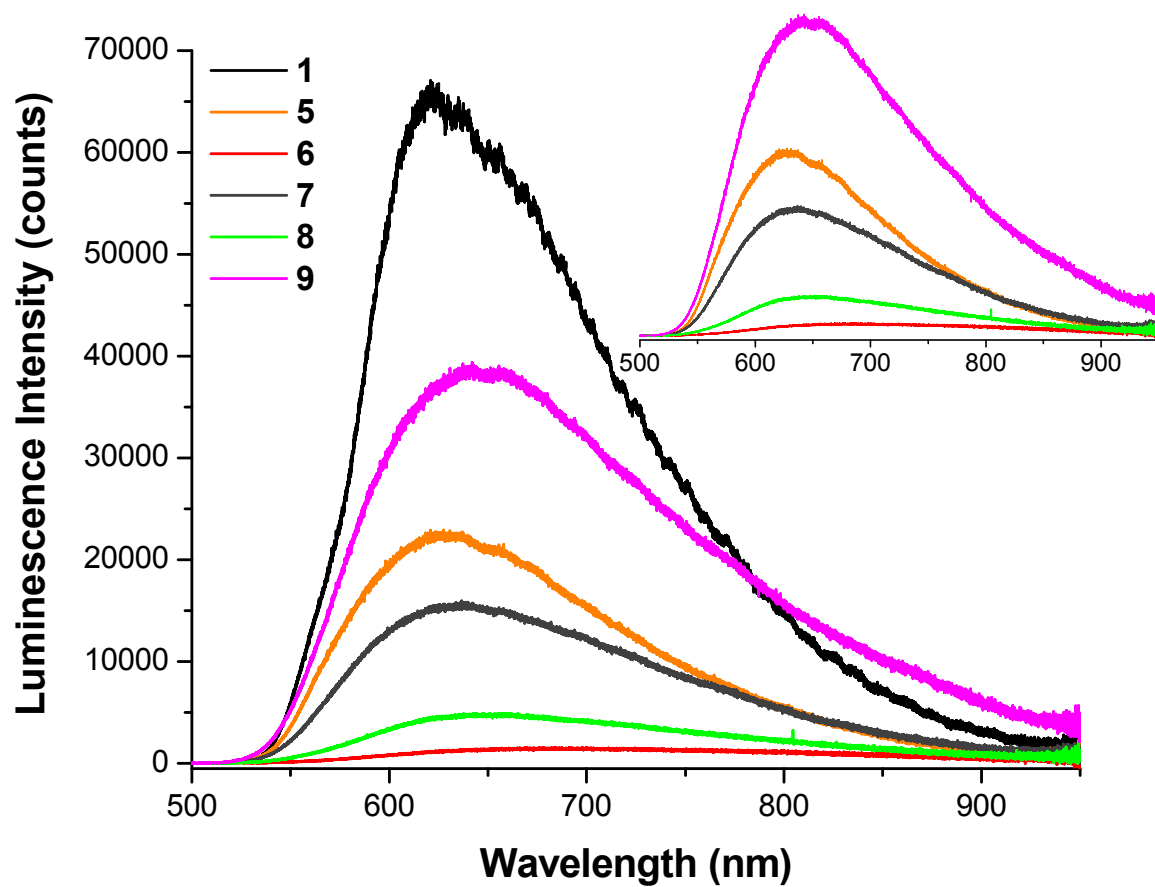


Fig. 6 Solid-state luminescence of mononuclear compounds

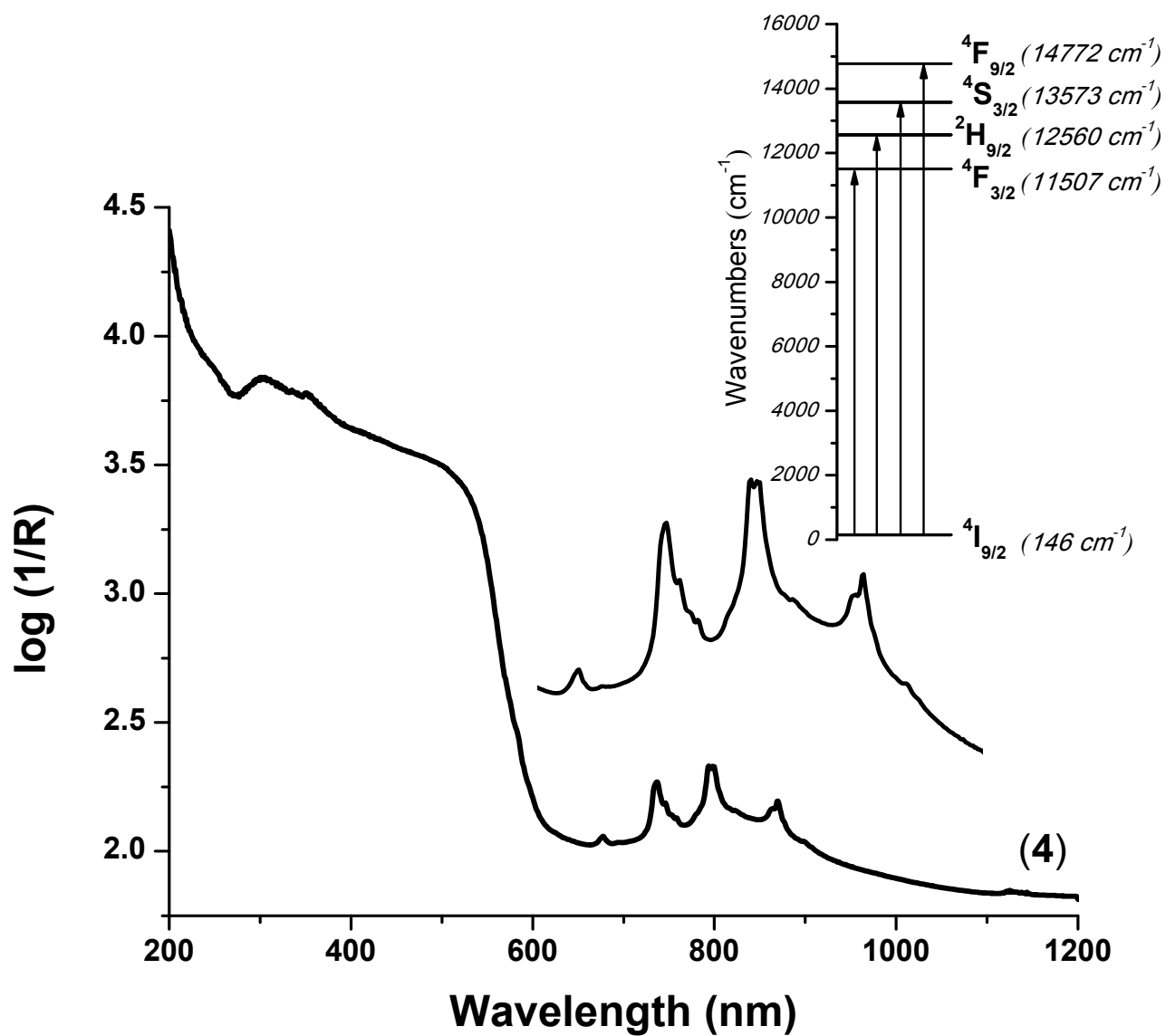


Fig. 7 Diffuse reflectance of $[Nd(ONO_2)_3(H_2L)] \cdot 1.5H_2O$

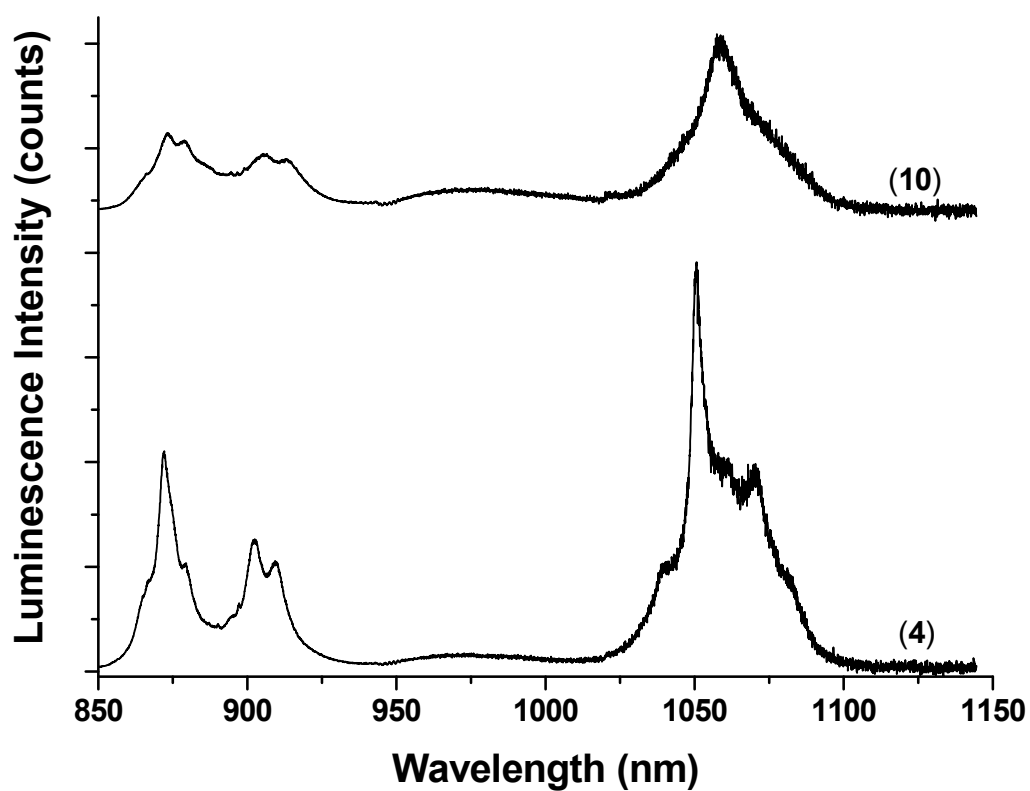


Fig. 8 Emission spectra of $[Nd(ONO_2)_3(L)] \cdot 1.5H_2O$ (**4**) and $[NdZn(ONO_2)_3(Cl)(L)(OH_2)] \cdot 2H_2O$ (**10**) at room temperature. λ_{ex} 488nm

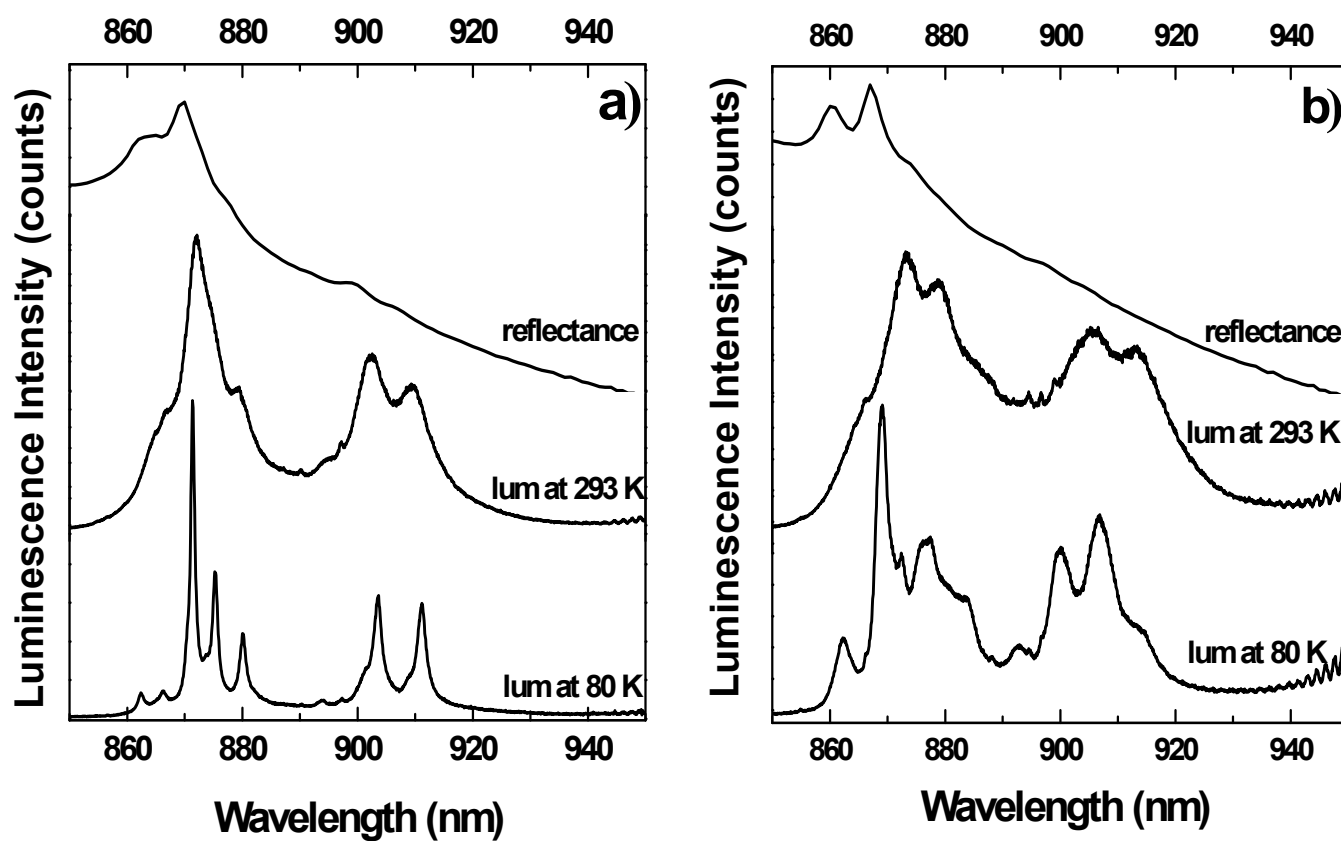


Fig. 9 Diffuse reflectance and luminescence spectra of left of $[Nd(ONO_2)_3(L)] \cdot 1.5H_2O$ (**4**) and right $[NdZn(ONO_2)_3(Cl)(L)(OH_2)] \cdot 2H_2O$ (**10**) at room temperature. λ_{ex} 488nm

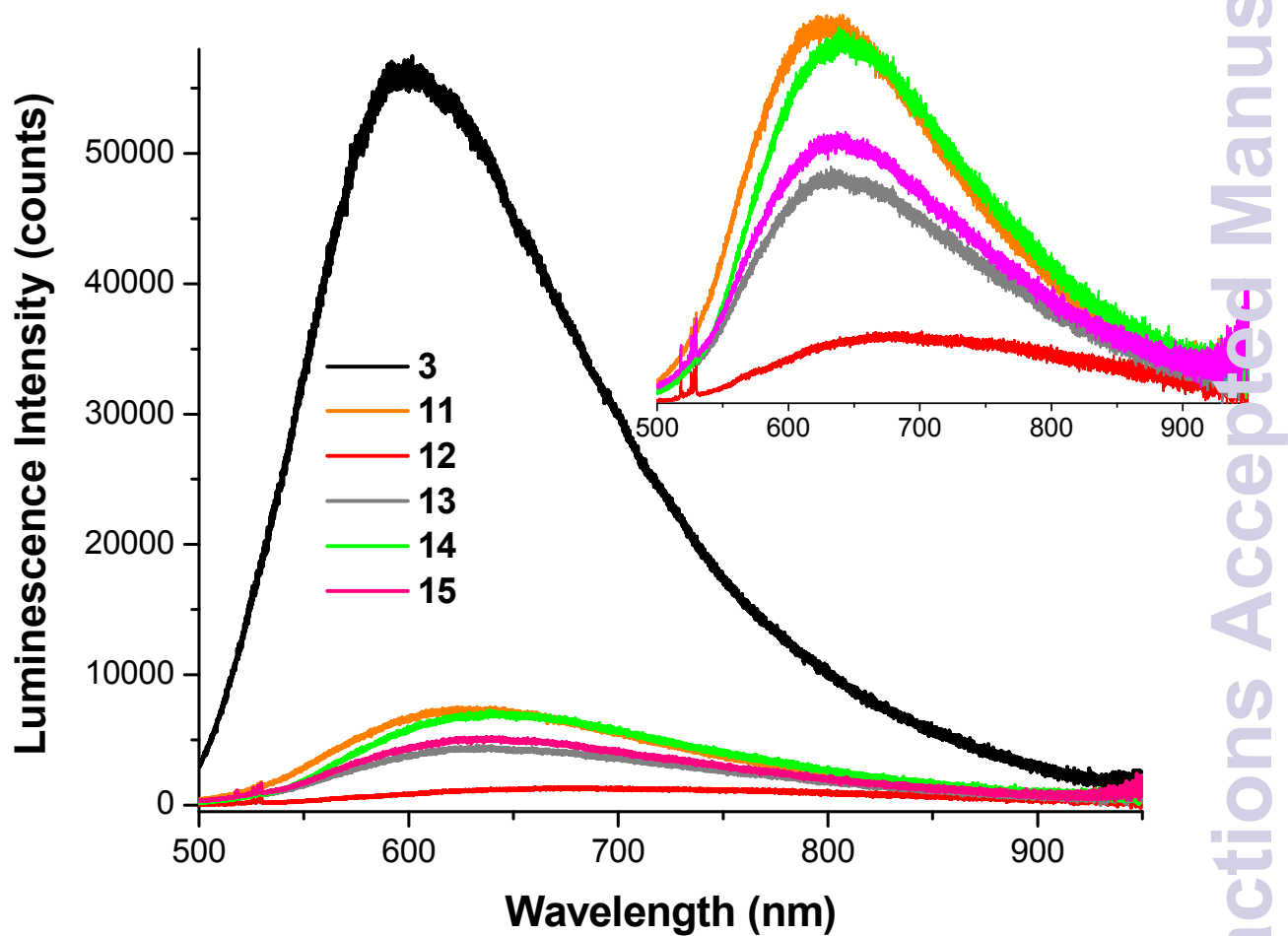


Fig. 10 Solid-state luminescence of dinuclear compounds

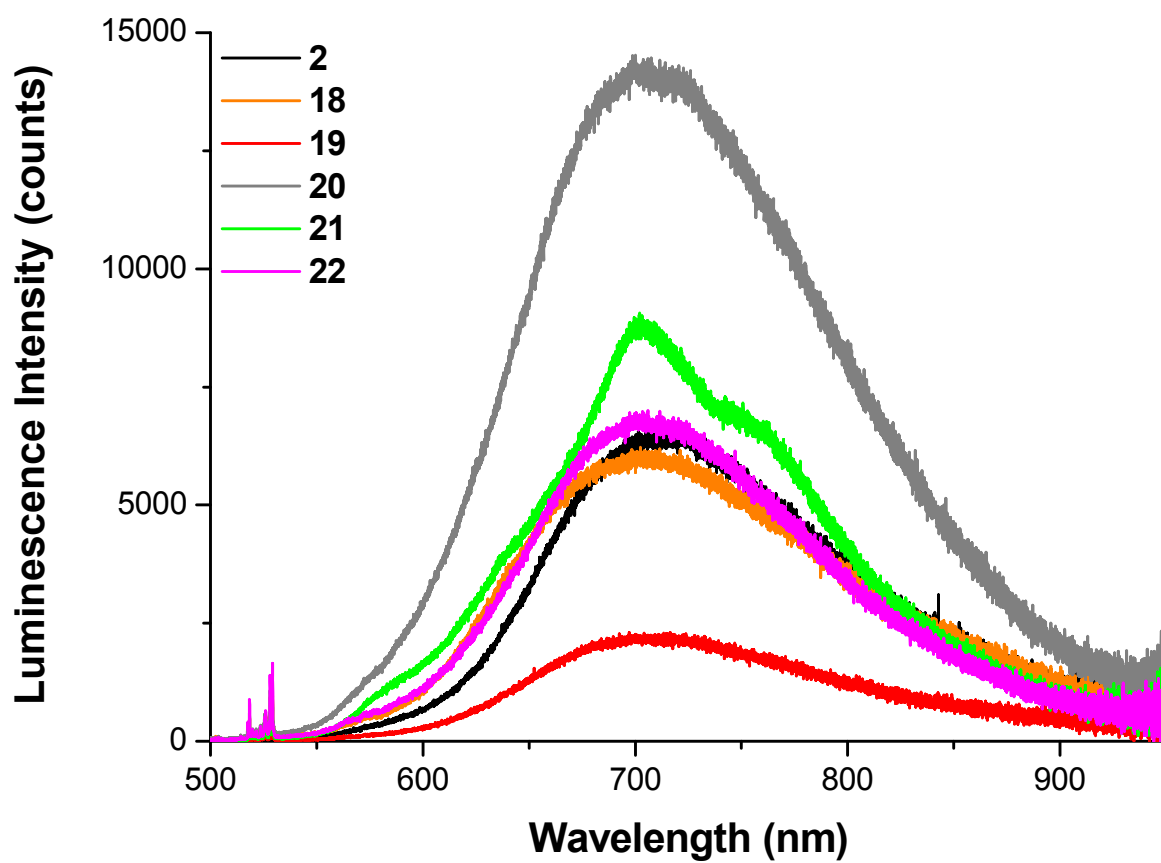


Fig. 11 Solid-state luminescence of trinuclear compounds